AD-A091 947 DAVID W TAYLOR NAVAL SHIP RESEARCH AND DEVELOPMENT CE--ETC F/G 20/11
RESPONSE OF A POINT EXCITED INFINITELY LONG CYLINDRICAL SHELL I--ETC(U)
NOV 80 W VOGEL, D FEIT

UNCLASSIFIED DTNSRDC-80/061 NL

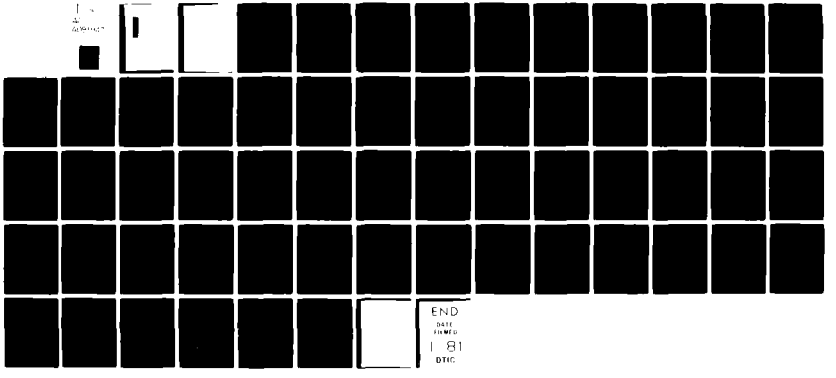

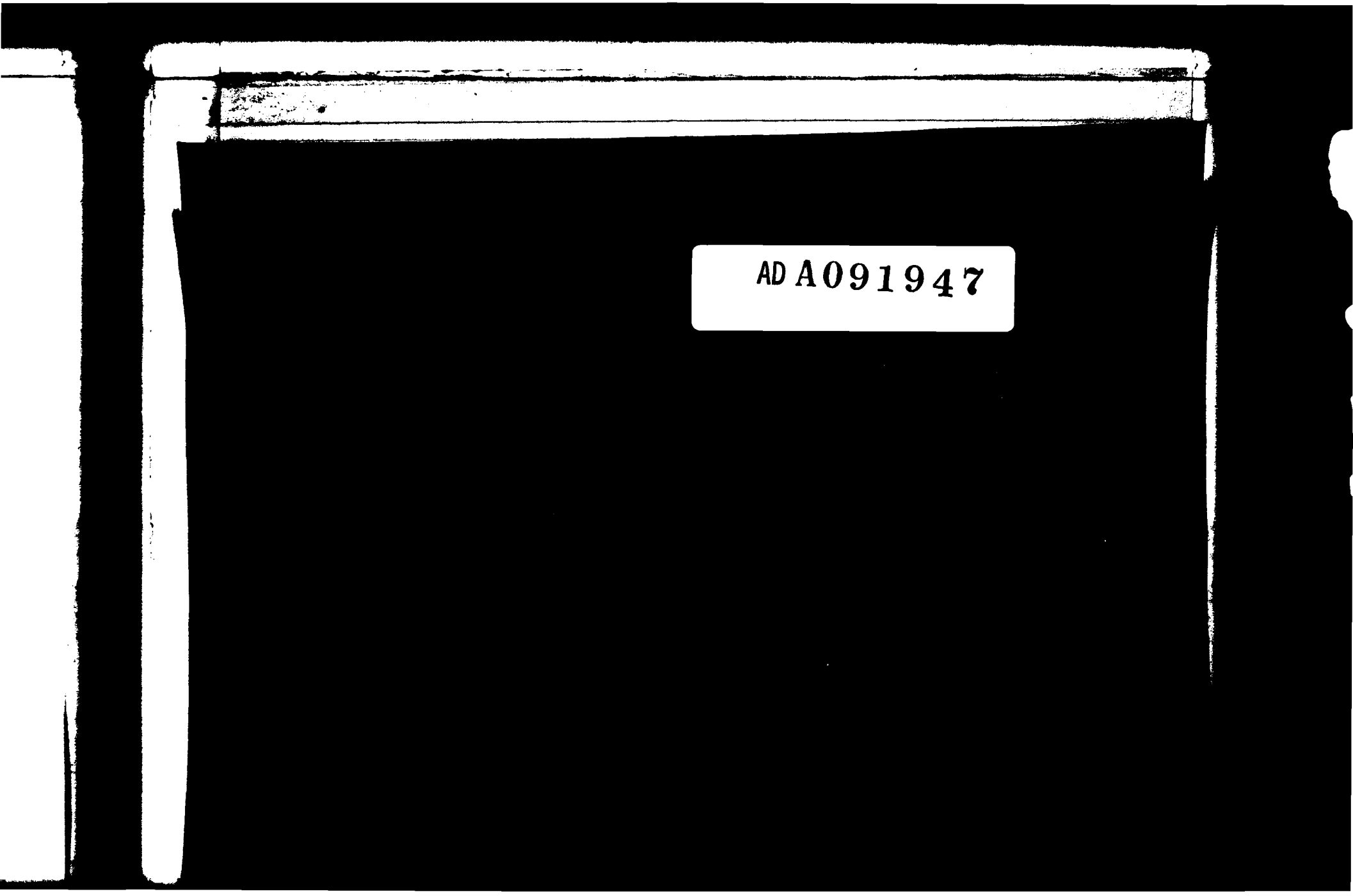

UNCLASSIFIED

SECURITY CLASSIFICATION OF THIS PAGE (When Data Entered)

REPORT DOCUMENTATION PAGE	READ INSTRUCTIONS BEFORE COMPLETING FORM
1. REPORT NUMBER: DTNSRDC-80/061 (14)	2. GOVT ACCESSION NO.: AD-A092 947
	3. RECIPIENT'S CATALOG NUMBER:
4. TITLE (and Subtitle): (6) RESPONSE OF A POINT EXCITED INFINITELY LONG CYLINDRICAL SHELL IMMERSED IN AN ACOUSTIC MEDIUM.	5. TYPE OF REPORT & PERIOD COVERED: Formal (16) F43452,
	6. PERFORMING ORG. REPORT NUMBER: ZR01108
7. AUTHOR(s): (10) William Vogel [redacted] David Feit (12) 62	8. CONTRACT OR GRANT NUMBER(s): (11) SF43452702, ZR0110801
9. PERFORMING ORGANIZATION NAME AND ADDRESS: David W. Taylor Naval Ship Research and Development Center, Bethesda, Maryland 20084	10. PROGRAM ELEMENT, PROJECT, TASK AREA & WORK UNIT NUMBERS: (See reverse side)
11. CONTROLLING OFFICE NAME AND ADDRESS: (9) Research and development Reports (11)	12. REPORT DATE: November 1980
	13. NUMBER OF PAGES: 58
14. MONITORING AGENCY NAME & ADDRESS (If different from Controlling Office): Naval Sea Systems Command (05H), Washington, D. C. 20360	15. SECURITY CLASS. (of this report): UNCLASSIFIED
	15a. DECLASSIFICATION/DOWNGRADING SCHEDULE:

16. DISTRIBUTION STATEMENT (of this Report)

APPROVED FOR PUBLIC RELEASE: DISTRIBUTION UNLIMITED

17. DISTRIBUTION STATEMENT (of the abstract entered in Block 20, if different from Report)

18. SUPPLEMENTARY NOTES

19. KEY WORDS (Continue on reverse side if necessary and identify by block number)

Point Driven Cylindrical Shell
Response of a Cylinder with Water Loading
Bending and Membrane Modes of a Cylindrical Shell
Point Driven Infinite Plate

20. ABSTRACT (Continue on reverse side if necessary and identify by block number)

The velocity distribution of a point excited, infinitely long, thin cylindrical shell immersed in an acoustic medium is considered. The problem is analyzed by applying integral transform techniques; a solution is then obtained by evaluating the inverse transform integrals numerically. Examples are presented to illustrate the effect of fluid loading on the vibrational behavior of a point excited cylindrical shell. In addition, results are compared with those of a point excited plate with and without fluid loading.

DD FORM 1 JAN 73 1473 EDITION OF 1 NOV 65 IS OBSOLETE
S/N 0102-LF-014-6601

UNCLASSIFIED

SECURITY CLASSIFICATION OF THIS PAGE (When Data Entered)

387682 slk

(Block 10)

Program Element 62543N
Task Area SF43452702
Work Units 1960-010 and 1960-020

TABLE OF CONTENTS

LIST OF FIGURES

Page

ABSTRACT

The velocity distribution of a point excited, infinitely long, thin cylindrical shell immersed in an acoustic medium is considered. The problem is analyzed by applying integral transform techniques; a solution is then obtained by evaluating the inverse transform integrals numerically. Examples are presented to illustrate the effect of fluid loading on the vibrational behavior of a point excited cylindrical shell. In addition, results are compared with those of a point excited plate with and without fluid loading.

ADMINISTRATIVE INFORMATION

The investigation presented in this report was initiated under the Independent Research Program, Program Element 61152N, Task Area ZR0110801, Work Unit 1960-011 and completed under funding from the Naval Sea Systems Command (05H) under Task Area SF43452702, Task 18185, Work Units 1960-010 and 1960-020.

INTRODUCTION

Understanding the vibration and radiation characteristics of a cylindrical shell is of considerable importance to the Navy. It can provide insight into the reasonableness of simplifying approximations currently utilized, for instance, determining the frequency range in which a complex structure can be modeled as a flat plate. Unfortunately, the analysis of a fluid loaded cylinder is complicated by the fact that there are three components of displacement which are coupled to each other. This differs from a flat plate where only one component of structural displacement is considered.

Determining a solution to the shell equations for an infinite cylinder is further complicated when fluid loading is included. However, the response of an infinite cylindrical shell with or without fluid loading can be determined, in theory, by applying integral transform techniques. The difficulty with this method is that complicated inverse transforms must be evaluated. Past studies have circumvented this difficulty by several approaches. One is to consider the exciting force specification to be independent of the coordinate defining the axial direction of the cylinder, which leads to a plane or two dimensional problem.[1*] Other investigators have simplified the problem by assuming an exciting force which is a periodic function having a specified axial wave length.[2,3] However, once a longitudinal wave length is specified, then only one longitudinal wave length is permitted for the response of the infinite cylinder. But in reality, all wave lengths are permissible for a point driven infinitely long cylindrical shell. Another configuration which avoids solving the inverse transform integrals is that of a cylindrical shell with periodic stiffeners which reduces the integral to a summation.[4] In any event, utilizing any of the above simplifying procedures negates to a varying degree the usefulness of the solution to the actual physical problem. On the other hand, with the use of large computers and refined numerical techniques, it is now possible to determine the response of a point excited fluid loaded cylinder or its radiated pressure directly, thus avoiding the above inhibiting assumptions.

---

*A complete listing of references is given on page 53.

FORMULATION OF PROBLEM

DESCRIPTION OF PROBLEM

The problem considered here consists of an infinitely long cylindrical shell with a radius "a" much larger than the shell wall thickness h. The cylinder is surrounded by an infinite fluid medium with a fluid density ρ and sound speed c. The cylinder is excited by a temporally varying point force $Fe^{-i\omega t}$ where F is the amplitude of the force and ω is the circular frequency of excitation. It will be assumed that the cylinder is in steady state vibration and therefore a time dependence of the form $e^{-i\omega t}$ for all dependent variables is assumed throughout the analysis.

The cylinder is defined by an r, ϕ, and z coordinate system where the r axis is directed outward along the normal to the shell's surface, ϕ defines the angle in the circumferential direction and z defines the longitudinal axis as shown in Figure 1. The above orthogonal displacements of the shell's middle surface are denoted by w, v and u, the radial, tangential, and longitudinal (or axial), respectively.

SHELL EQUATIONS OF MOTION

For a thin cylindrical shell the equations of motion are

$$\frac{\partial^2 u}{\partial z^2} + \frac{1-\nu}{2a^2}\frac{\partial^2 u}{\partial \phi^2} + \frac{1+\nu}{2a}\frac{\partial^2 v}{\partial z \partial \phi} + \frac{\nu}{a}\frac{\partial w}{\partial z} - \frac{\ddot{u}}{c_p^2} = 0 \qquad \text{(1a)}$$

$$\frac{1+\nu}{2a}\frac{\partial^2 u}{\partial z \partial \phi} + \frac{1-\nu}{2}\frac{\partial^2 v}{\partial z^2} + \frac{1}{a^2}\frac{\partial^2 v}{\partial \phi^2} + \frac{1}{a^2}\frac{\partial w}{\partial \phi} - \frac{\ddot{v}}{c_p^2} = 0 \qquad \text{(1b)}$$

$$\frac{\nu}{a}\frac{\partial u}{\partial z} + \frac{1}{a^2}\frac{\partial v}{\partial \phi} + \frac{w}{a^2} + \beta^2\left(a^2\frac{\partial^4 w}{\partial z^4} + 2\frac{\partial^4 w}{\partial z^2 \partial \phi^2} + \frac{1}{a^2}\frac{\partial^4 w}{\partial \phi^4}\right)$$

$$+ \frac{\ddot{w}}{c_p^2} - \frac{p_a(1-\nu^2)}{Eh} = 0 \qquad (1c)$$

where $c_p = \sqrt{\dfrac{E}{\rho_s(1-\nu^2)}}$, the compressional wave velocity in an elastic plate

E = Young's modulus

ν = Poisson's ratio

ρ_s = mass density of shell material

$\beta = \dfrac{h}{\sqrt{12}\,a}$

h = shell wall thickness

p_a = total pressure acting on shell

a = radius of cylindrical shell

The total pressure acting on the shell can be expressed as

$$p_a = \frac{F\delta(z)\delta(\phi)e^{-i\omega t}}{a} - p(a,\phi,z,t) \qquad (2)$$

where

$$p(a,\phi,z,t) = p_o(a,\phi,z)e^{-i\omega t}$$

$\delta(\phi)$ = delta function with argument ϕ

The first term on right hand side of Equation (2) is due to the harmonically varying point force whereas the second term is due to the fluid pressure acting on the shell surface.

The motion of the shell can be described by assuming displacements of the form

$$u(\phi,z,t) = \sum_{n=0}^{\infty} \cos n\phi \; U_n(z) e^{-i\omega t} \tag{3a}$$

$$v(\phi,z,t) = \sum_{n=0}^{\infty} \sin n\phi \; V_n(z) e^{-i\omega t} \tag{3b}$$

$$w(\phi,z,t) = \sum_{n=0}^{\infty} \cos n\phi \; W_n(z) e^{-i\omega t} \tag{3c}$$

FOURIER TRANSFORM METHOD OF SOLUTION

Solutions to problems of the type considered here, that is, systems described by independent variables extending over an infinite domain, are greatly facilitated by employing integral transform techniques. The Fourier transform pair which will be used in this analysis is defined

$$F(k) = \int_{-\infty}^{+\infty} e^{-ikz} \; f(z)dz \tag{4}$$

which transforms the f(z) into the wave number domain, and the inverse transform,

$$f(z) = \frac{1}{2\pi} \int_{-\infty}^{+\infty} e^{ikz} F(k)dk \tag{5}$$

which transforms the function F(k) back into the spatial domain.

Substituting Equation (3) into Equation (1) and transforming the result into the wave number domain yields

$$\left[k^2a^2 + \frac{(1-\nu)}{2} n^2 - \Omega^2\right] U_n(k) - ikan\frac{(1+\nu)}{2} V_n(k) - ika\nu W_n(k) = 0 \tag{6a}$$

$$ika n \frac{(1+\nu)}{2} U_n(k) + \left[k^2 a^2 \frac{(1-\nu)}{2} + n^2 - \Omega^2 \right] V_n(k) + n W_n(k) = 0 \qquad (6b)$$

$$ika\nu U_n(k) + n V_n(k) + \left[\beta^2 (k^2 a^2 + n^2)^2 + 1 - \Omega^2 \right] W_n(k)$$

$$= \int_0^{2\pi} \frac{\varepsilon_n}{2\pi} a^2 \frac{(1-\nu^2)}{Eh} \left[\frac{F\delta(\phi)}{a} - P(a,\phi;k) \right] \cos n\phi \, d\phi \qquad (6c)$$

where $\Omega = \frac{\omega a}{c_p}$ is a nondimensionalized frequency parameter.

The above equations were obtained by utilizing the orthogonality conditions

$$\frac{\varepsilon_n}{2\pi} \int_0^{2\pi} \cos m\phi \cos n\phi \, d\phi = \delta_{mn} \qquad (7a)$$

$$\frac{1}{\pi} \int_0^{2\pi} \sin m\phi \sin n\phi \, d\phi = \delta_{mn} \qquad (7b)$$

where

$$\delta_{nm} = \begin{cases} 1 & n=m \\ 0 & n \neq m \end{cases} \quad \text{and} \quad \varepsilon_n = \begin{cases} 1 & n=0 \\ 2 & n \geq 1 \end{cases}$$

The term $F\delta(\phi)$ on the right hand side of Equation (6c) due to the exciting force can be expanded in terms of a Fourier series, i.e.

$$F\delta(\phi) = \sum_{n=0}^{\infty} F_n \cos n\phi \qquad (8)$$

Multiplying both sides by cos $m\phi d\phi$ and integrating between 0 and 2π yields

$$F_n = \frac{\epsilon_n}{2\pi} \int_0^{2\pi} F\delta(\phi) \cos m\phi d\phi = \frac{\epsilon_n}{2\pi} F \tag{9}$$

Consequently, from Equations (8) and (9)

$$F\delta(\phi) = \sum_{n=0}^{\infty} \frac{F\epsilon_n}{2\pi} \cos n\phi \tag{10}$$

PRESSURE DUE TO FLUID MEDIUM

The term $P(a,\phi,k)$ in Equation (6c) is the Fourier transform of the pressure acting on the shell due to the presence of the fluid medium. This term can be related to the radial motion of the shell by utilizing the wave equation governing the fluid medium and the appropriate boundary condition at the fluid-shell interface. The wave equation in cylindrical coordinates is

$$\nabla^2 p(r,\phi,z,t) - \frac{1}{c^2} \frac{\partial^2 p(r,\phi,z,t)}{\partial t^2} = 0 \tag{11}$$

where

$$\nabla^2 = \frac{\partial^2}{\partial r^2} + \frac{1}{r} \frac{\partial}{\partial r} + \frac{1}{r^2} \frac{\partial^2}{\partial \phi^2} + \frac{\partial^2}{\partial z^2}$$

$$p(r,\phi,z,t) = p_o(r,\phi,z)e^{-i\omega t}$$

Suppressing the harmonic time dependence the wave equation can be written as

$$\nabla^2 p_o(r,\phi,z) + k_o^2 p_o(r,\phi,z) = 0 \tag{12}$$

where $k_o = \frac{\omega}{c}$ is the wave number of the acoustic medium.

To determine the transformed pressure $P_o(a,\phi;k)$ the z domain in the wave equation is transformed into the wave number domain.

$$\left(\frac{\partial^2}{\partial r^2} + \frac{1}{r}\frac{\partial}{\partial r} + \frac{1}{r^2}\frac{\partial^2}{\partial \phi^2} + k_o^2 - k^2\right) P_o(r,\phi;k) = 0 \tag{13}$$

Since the fluid medium is infinite in extent, there are only waves propagating outward from the cylinder. Therefore, the solution to the above differential equation is the Hankel Function of the first kind; thus

$$P_o(r,\phi;k) = \sum_{n=0}^{\infty} A_n H_n \left[(k_o^2 - k^2)^{1/2} r\right] \cos n\phi \tag{14}$$

The constant A_n can be determined from the boundary condtion at the fluid-shell interface where continuity requires the shell and fluid particle velocity to be equal, i.e.,

$$\frac{\partial w}{\partial t}(\phi,z,t) = v_f(r,\phi,z,t)\Big|_{r=a} \tag{15}$$

The fluid particle velocity v_f is related to the fluid pressure by the momentum balance relation

$$\frac{\partial p}{\partial r}(r,\phi,z,t) = -\rho \frac{\partial v_f}{\partial t}(r,\phi,z,t) \tag{16}$$

Combining Equations (15) and (16) while suppressing the harmonic time dependence we have

$$\frac{\partial p_o}{\partial r}(r,\phi,z)\Big|_{r=a} = -i\rho\omega \dot{w}_o(\phi,z) = \rho\omega^2 w_o(\phi,z) \tag{17}$$

where

$$w(\phi,z,t) = w_o(\phi,z)e^{-i\omega t}$$

In the wave number domain the above equation can be expressed as

$$\frac{\partial P_o}{\partial r}(r,\phi;k) = \rho\omega^2 w_o(\phi;k) \tag{18}$$

where

$$w_o(\phi;k) = \sum_{n=0}^{\infty} \cos n\phi \; W_n(k)$$

Combining Equations (14) and (18) and solving for A_n one obtains

$$A_n = \frac{\rho\omega^2 W_n(k)}{H_n'\left[(k_o^2 - k^2)^{1/2} a\right]\left[k_o^2 - k^2\right]^{1/2}}$$

Consequently,

$$P_o(r,\phi;k) = \sum_{n=0}^{\infty} Z_{nr}(k)\ \dot{W}_n(k)\ \cos n\phi \tag{19a}$$

where

$$Z_{nr}(k) = \frac{i\rho c k_o H_n\left[(k_o^2 - k^2)^{1/2} r\right]}{(k_o^2 - k^2)^{1/2} H_n'\left[(k_o^2 - k^2)^{1/2} a\right]} \tag{19b}$$

is the transform of the fluid impedance. The transform of the fluid pressure, $p(a,\phi,z)$ acting on the shell surface is obtained by setting r=a. Thus

$$P_o(a,\phi;k) = \sum_{n=0}^{\infty} Z_{na}(k)\ \dot{W}(k)\ \cos n\phi \tag{20a}$$

where

$$Z_{na}(k) = \frac{i\rho c k_o H_n\left[(k_o^2 - k^2)^{1/2} a\right]}{(k_o^2 - k^2)^{1/2}\left[H_n'\ (k_o^2 - k^2)^{1/2} a\right]} \tag{20b}$$

DETERMINATION OF CYLINDER'S RADIAL RESPONSE

Substituting the transformed expressions for the exciting force and fluid pressure acting on the cylinder into Equation (6c) yields

$$- ika\nu U_n(k) + n\ V_n(k) + \left[\beta^2(k^2a^2+n^2)^2 + 1 - \Omega^2 - a^2\ \frac{(1-\nu^2)}{Eh}\ i\omega Z_{na}(k)\right] W_n(k)$$

$$= \frac{a(1-\nu^2)\varepsilon_n\ F}{2\pi\ Eh} \tag{21}$$

The radial component $W_n(k)$ can now be determined from Equations (6a), (6b) and (21) by applying Cramer's rule, i.e.,

$$W_n(k) = \frac{\varepsilon_n F}{-i\omega 2\pi a \left[Z_{np}(k) + Z_{nm}(k) + Z_{na}(k)\right]} \tag{22a}$$

where

$$Z_{np}(k) = \frac{i\, c_p \rho_s\, h}{\Omega a}\left[\beta^2(a^2k^2 + n^2)^2 + 1 - \Omega^2\right] \tag{22b}$$

$$Z_{nm}(k) = \frac{i\, c_p \rho_s\, h}{\Omega a}\left\{\frac{k^2a^2\nu\left[n^2(1+\nu) + \nu(\Omega^2 - k^2a^2(1-\nu)/2 - n^2)\right]}{DEN} + \frac{n^2\left[\Omega^2 - (1-\nu)\, n/2 - k^2a^2\right]}{DEN}\right\}$$

$$DEN = \left[\Omega^2 - \frac{(1-\nu)n^2}{2} - a^2k^2\right]\left[\Omega^2 - a^2k^2\,\frac{(1-\nu)}{2} - n^2\right] - k^2a^2n^2\,\frac{(1+\nu)^2}{4} \tag{22c}$$

$Z_{np} + Z_{nm}$ describes the impedance of the entire cylindrical shell. Note that Z_{np} approaches the impedance of a plate as Ω approaches ∞. On the other hand, Z_{nm}, the impedance due to the membrane terms of the cylindrical shell, approaches zero when $\Omega >> 1$.

By applying the inverse Fourier transform,

$$W_n(z) = \frac{1}{2\pi}\int_{-\infty}^{+\infty} W_n(k) e^{ikz} dk \tag{23}$$

to Equation (19) and substituting the result into Equation (3c), the radial velocity of the cylinder can be expressed as

$$\dot{w}(\phi,z,t) = \frac{F}{(2\pi)^2 a}\sum_{n=0}^{\infty}\varepsilon_n \cos n\phi e^{-i\omega t}\int_{-\infty}^{+\infty} G_n(k)dk \qquad (24a)$$

where

$$G_n(k) = \frac{e^{ikz}\,dk}{Z_{np}(k) + Z_{nm}(k) + Z_{na}(k)} \qquad (24b)$$

Similar expressions can be obtained for the displacements u and v.

RADIATED PRESSURE FIELD

The radiated pressure field can now be expressed as

$$p(r,\phi,z,t) = \frac{F}{(2\pi)^2 a}\sum_{n=0}^{\infty}\varepsilon_n \cos n\phi e^{-i\omega t}\int_{-\infty}^{+\infty} Z_{nr}(k)G_n(k)dk \qquad (25)$$

where $Z_{nr}(k)$ and $G_n(k)$ are defined by Equations (19b) and (24b), respectively.

Referring to the expressions for Z_{nr} (or Z_{na}) it can be seen that for $k_o > k$, Z_{nr} has both a real (resistive) and imaginary (reactive) part. Thus for $k_o > k$ energy will be radiated into the acoustic medium. On the other hand, when $k > k_o$ the arguments of Z_{nr} become imaginary and the Hankel function can be replaced by the modified Hankel function with a real argument, namely,

$$H_n(ix) = \frac{2}{\pi} i^{-(n+1)} K_n(x) \qquad (26)$$

Therefore for $k>k_o$

$$Z_{nr}(k) = \frac{\rho c k K_n\left[\left(k^2 - k_o\right)^{1/2} r\right]}{\left(k^2 - k_o^2\right)^{1/2} K_n'\left[\left(k^2 - k_o^2\right)^{1/2} a\right]} \tag{27}$$

which is purely a reactive and mass-like impedance. Thus for $k>k_o$ no energy will be radiated.

METHOD OF SOLUTION

The integral in Equation (24a) may be referred to as a modal influence function which relates the response of the cylinder at a point z due to a force applied in this case at z=0 for a particular mode n. Similarly the integral in Equation (25) relates the radiated pressure to the force for a particular mode n. The total response or radiated pressure is then obtained by summing the modal functions for all the circumferential modes.

There is no known closed form solution to the above integrals. The integrands are transcendental functions further complicated by the presence of poles and branch points in the complex k plane. The integrand is not analytic for all values of k in the complex k plane. The technique employed to evaluate the modal functions is similar to the one developed for evaluating the Green's function for a line driven, fluid loaded infinite plate. This method involves numerically evaluating the inverse Fourier transform integrals along the real axis after structural damping has been introduced into the integrand. Structural damping is introduced by replacing Young's modulus E by $E(1-i\eta)$ and is necessary to move the singularities off the real axis. η is the loss factor for the shell material. Briefly, the numerical scheme is based on using variable integration increments along

the path of integration. The size of the increment is automatically adjusted so as to keep the incremental change of the integrand values within prescribed limits. In essence, the second derivative of the function controls the mesh size. Thus where the integrand is not well behaved near a singularity the mesh size is very fine. On the band where the integrand is well behaved the mesh size is much larger. This method produces a set containing a minimum number of integration points which accurately describes the function to be integrated in a very smooth and continuous fashion. Once the set of points has been generated, the integral is evaluated by using Simpson's rule.

DISCUSSION OF RESULTS

The results presented in this report are for a shell thickness to radius ratio of h/a=.01. Response calculations were performed for both the in vacuo and water loaded cases. In order to put the results into perspective, they are compared with those of an equivalently loaded plate. This is particularly important, since an analysis of this type for a point excited cylindrical shell has apparently never been previously published.

MODAL RESPONSE OF CYLINDRICAL SHELL

The total response of a cylinder is a summation over all its modal responses. In practice, however, only a finite number of modes have to be summed. The number of modes to be summed depends primarily on the excitation frequency and the degree of accuracy desired. Consequently, it is informative to see how individual circumferential modes vary as a function of frequency and also the relative contribution of the various modes when the cylinder is excited at a particular frequency.

The results presented in this section all have been normalized to an equivalent line loaded plate. The drive point velocity of a line loaded infinite plate in vacuo has an exact solution of the form

$$G_p(o) = \frac{F'k_p}{4\omega m}(1+i\eta)^{1/4}(1+i) \simeq \frac{F'k_p}{4\omega m}(1+i\eta/4)(1+i) \qquad (28)$$

The normalizing factor is $F'k_p/4\omega m$ where $F' = F/2\pi a$ has the units of force per unit length and F is the point force acting on the cylinder.

In Figure 2, the real and imaginary components of the admittance in vacuo for the n=0 circumferential mode are shown as a function of the frequency parameter α. The frequency parameter α is often used for plates and is equal to k_o/k_p where k_o is the acoustic wave number of the acoustic medium and k_p is the plate wave number. Also, α is equal to $(\omega/\omega_c)^{1/2}$ where ω_c is the coincident frequency of the plate. In terms of the non-dimensionalized frequency parameter Ω, $\alpha = (c_p/c)(\Omega\beta)^{1/2}$.

Referring to Figure 2 the maximum response as a function of frequency, a resonance, for the n=0 occurs at the ring frequency of the cylindrical shell. That is when the compressional structureborne wave length in the shell material equals the circumference of the cylinder. In vacuo the ring frequency is given by $f_o = c_p/2\pi a$. Above the ring frequency, the admittance converges rapidly to the admittance of a line excited plate which has a normalized value of .975 + i1.025 with a loss factor of .1. For n=0 the tangential component of motion for the shell is zero.

In Figure 3, the real and imaginary components of the admittance of the n=0 mode and a line excited plate are compared with water loading included. As in the in vacuo case, the cylindrical shell admittance differs considerably from that of a line driven plate in the vicinity of the ring

frequency of the cylinder. However, the amplitude at resonance is much lower with fluid loading than the corresponding in vacuo case. This is due to the fact that at the ring frequency the structural wave length is larger than the acoustic wave length in the fluid and consequently the n=0 mode of a cylinder is a very efficient radiator at this frequency and is strongly damped by radiation.

In addition, the presence of the fluid lowers the nondimensionalized frequency of the n=0 mode from $\Omega=1$ for the in vacuo case to $\Omega \simeq .77$ with fluid loading. Junger and Feit have obtained an expression for approximating the natural frequency of the n=0 mode of a submerged cylindrical shell.[5] The approximation is

$$\Omega = \left[1 + \left(\frac{\rho}{\rho_s k_p h}\right)\right]^{-1/2}$$

It is reassuring to note that the above expression predicts that the reduced ring frequency of the n=0 mode in water to be $\Omega \simeq .77$.

In Figure 4 the admittance corresponding to circumferential mode number 6 is shown as a function of frequency with and without water loading. Unlike the n=0 circumferential mode there are now two resonant frequencies. As a matter of fact for each n>1 there are always two resonant frequencies present in the radial response. The lower resonant frequency is primarily an inextensional type mode where as the higher resonant frequency is primarily an extensional or membrane type mode.

In Figure 5 the drive point response of the forty first circumferential mode is illustrated as a function of frequency with water loading included. Again there are two resonant frequencies. However, unlike the case for low

values of n, there is very little radial motion due to extentional or membrane strains at the higher resonant frequency. This difference can be explained by energy considerations.[6] Arnold and Warburton have shown that at low circumferential wave numbers n/a, the strain energy associated with bending is low compared to the strain energy due to stretching of the reference surface. On the other hand, at higher circumferential wave numbers the bending strain energy is high whereas the stretching strain energy is low.

Since the response of the cylinder depends upon all the circumferential modes of vibration, it is of interest to see how each individual mode contributes to the total response when the cylinder is excited at a particular frequency. Figure 6 demonstrates the relative contribution of the various modes when the cylinder is driven at a frequency near the resonance frequency corresponding approximately to the forty first bending mode. As can be expected, the modes in the vicinity of the resonant bending mode contribute substantially more to the radial response than do modes farther away. The radial response of the cylinder at this exciting frequency would be primarily due to circumferential bending rather than stretching of the reference surface. It can also be shown that for values of n somewhat larger than the predominantly excited modes, the admittance decreases at the rate of $1/n^3$ (see Appendix B). Thus it is relatively easy to minimize truncation errors when calculating the drive point admittance.

RESPONSE OF A POINT EXCITED CYLINDER

As previously pointed out the response of a point excited cylinder should converge at higher frequencies to that for a point excited plate. Thus, for convenience, the results in this section are normalized to the

admittance of a point driven plate in vacuo (see Appendix A). In vacuo, the velocity of a point excited plate at radius r can be expressed as

$$v_v(r) = \frac{F}{2\pi} \int_0^{+\infty} \frac{kJ_o(rk)dk}{Z_p(k)} \tag{29}$$

and with fluid loading, the velocity is

$$v_f(r) = \frac{F}{2\pi} \int_0^{+\infty} \frac{kJ_o(rk)dk}{Z_p(k) + Z_a(k)} \tag{30}$$

where J_o = cylindrical Bessel function of zero order

$Z_p(k)$ = is the transform of the plate surface impedance operator

$Z_a(k)$ = is the transform of the fluid impedance

r = distance from the applied force

It can be shown that the admittance or drive point velocity (r=0) of the plate in vacuo is independent of frequency and can be expressed as

$$v_v(0) = \sqrt{\frac{3}{4}} \frac{F}{\rho_s c_p h^2} \tag{31}$$

The above term is used to normalize all results presented in this section. The velocity response away from the drive point for the in vacuo and fluid loading cases are obtained by numerically integrating Equations (29) and (30), respectively, by a method similar to the one outlined for a cylinder. In the case of fluid loading the admittance must also be obtained numerically.

In Figure 7 the normalized admittance for a point excited cylinder is shown with and without water loading as a function of the frequency parameter α. These results are compared with the admittance of a point

driven plate. Since the admittance of a plate in vacuo is independent of frequency, its normalized value is therefore a constant equal to one. As should be expected, the greatest difference between a plate and cylindrical shell occurs in the vicinity of the ring frequency and at lower frequencies. However, it is surprising how quickly the admittance of the cylinder converges to a plate for both the in vacuo and fluid loaded cases. Nevertheless, the frequency at which the admittance of a point driven cylinder approaches that of a plate depends on the parameter h/a. For values of h/a larger than used here, the frequency would be higher. On the other hand, for smaller values of h/a the convergence frequency would be lower.

The peaks in the admittance curves occur at frequencies corresponding to the ring frequency of the cylinder. The response at this frequency is dominated by the n=0 mode. At lower frequencies, i.e., low values of α, the admittance curves for the cylinder are shown as smooth functions of α for convenience only. To further explain this, let us assume that the response of the cylinder has no z dependence; then the natural frequencies of the circumferential bending modes in vacuo are given by

$$f_n \simeq \frac{c_p}{2\pi} \frac{\beta n}{a} \frac{(n^2+1)}{(n^2-1)^{1/2}} \qquad (32)$$

The above relation can also be used to approximate exciting frequencies which are half way between any two adjacent circumferential bending modes of the cylinder. Figure 8 illustrates the effect on the velocity response when the exciting frequency coincides with the frequency of a resonant bending mode (n=integer) and when it does not (for instance when n=integer + .5). As can be seen from the figure there is an oscillation

in the response at lower frequencies. However, as the frequency increases, the disparity becomes less and less until the response curve becomes smooth regardless of the exciting frequency. This is because the circumferential bending waves are dispersive and their wave lengths become smaller as the exciting frequency increases. Consequently, at higher frequencies the waves damp out more quickly, thus eliminating any reinforcement or cancellation which would tend to occur at lower frequencies. It should be pointed out, however, that the rate at which the envelope closes depends on the damping value.

Figures 9 and 10 demonstrate the differences in the velocity profile away from the drive point between a plate and cylinder when excited at the ring frequency of a cylinder without and with water loading, respectively. For the cylinder the velocity profile is along the z axis and the distance from the drive point is expressed in nondimensionalized form as z/a. Figures 9 and 10 show considerable differences in the velocity profiles between a point driven plate and cylinder, particularly for the in vacuo case. This should be expected since, at the ring frequency, the radial motion of the cylinder is primarily due to extensional strains of the shell's middle surface. However, water loading does moderate the differences in the velocity profile between a point driven plate and a cylinder. In any event, as the admittance of a point driven plate and cylinder approach each other at higher frequencies, one would also expect their respective velocity profiles in the vicinity of the drive point to become increasingly similar. The degree of similarity will depend not only on the exciting frequency but also on the amount of damping, for it is the damping value which determines how quickly the propagating waves from the drive

point decay and therefore how localized the vibration pattern becomes. The more localized the vibration pattern is, the less is the effect the shell curvature has upon the vibration response.

Figure 11 illustrates the resulting velocity profile in vacuo around the circumference of the cylinder when the excitation frequency coincides with the ring frequency of the cylinder. At the ring frequency, the response of the cylinder is a combination of the predominantly excited bending modes superimposed upon the predominantly excited membrane modes. Figure 12 illustrates the contribution of the various modes to the total drive point response at the ring frequency. The resonant peak that occurs at the lower mode numbers is due to the resonant membrane modes as well as the rigid body mode (n=1). On the other hand, the second peak is due to a resonant bending mode. The dominant resonant bending mode has an n value of 18. This mode has a structural wavelength that corresponds to an angle of 20 degrees along the circumference of the cylinder. As a result, the lobes in the response occur at approximately 20^{o} intervals. If fluid loading is included (Figure 13), the response at the ring frequency is not only substantially reduced but the lobes rapidly disappear away from the drive point. This can be attributed to the fact that in fluid the excited membrane modes of the cylinder are critically damped due to radiation. To further illustrate this, the contribution of each mode to the total drive point response with fluid loading is shown in Figure 14. A comparison with the in vacuo case, Figure 12, clearly demonstrates that the presence of the fluid greatly reduces the amplitude of the resonant peak due to the resonant membrane modes and the rigid body mode. This reduction takes place because these modes are efficient radiators and therefore lose energy through radiation damping.

Figures 15 and 16 compare the velocity response of a cylinder and plate away from the drive point along the generator without and with water loading, respectively, at an exciting frequency corresponding to $\alpha=.5$. As the two figures indicate, at $\alpha=.5$ the response of a plate and cylinder are identical at least for the range of z/a where calculations were performed. Thus, for the values of h/a and damping used here, the vibration response of a cylinder can, for all practical purposes, be accurately represented by a flat plate in the vicinity of $\alpha=.5$.

Figures 15 and 16 also illustrate the velocity response of a point driven plate excited at a frequency of $\alpha=1.5$ with and without water loading, respectively. In view of the results for $\alpha=.5$, the velocity response of a point driven cylinder should be and in fact is identical to a point driven plate for $\alpha=1.5$.

So far only the velocity response along the z axis of the cylinder has been compared with that of a point driven plate of equivalent radius r. Indeed, if at some frequency a cylinder can be approximated by a plate, the velocity response along the circumference of a cylinder away from the drive point should also be similar to a point driven plate. In Figure 17 such a comparison is made between a point driven cylinder and plate with $\alpha=.5$. From Figure 17 it is obvious that the two responses are indeed very similar for the range of z/a considered and for a damping value of .1.

Figure 18 demonstrates how localized the velocity pattern near the drive point becomes with $\alpha=.5$. In Figure 18 a 10^{o} increment corresponds to a z/a increment of approximately .175 in Figure 17.

All the previous results have been arrived at by assuming a damping factor .1. Although a damping factor of .1 may be a reasonable value

for many structures, it may be too high for others. Consequently, in order to demonstrate the effect of structural damping on the vibration response of a cylinder, calculations were also performed using a very small damping value of .01. In Figure 18 the velocity envelope around the circumference of a cylinder is shown when the excitation frequency corresponds to the ring frequency in vacuo. A comparison between Figures 11 and 19 demonstrates how the velocity envelope becomes more complicated when the damping value is changed from .1 to .01. This is due to the fact that structural waves generated at the drive point do not damp out as rapidly and thus travel around the circumference of the cylinder in opposite directions with larger amplitudes. Consequently when the two waves meet, they either reinforce or interfere with each other depending on the observation point on the circumference of the cylinder. As previously pointed out, the predominantly excited bending mode at the ring frequency in vacuo is n=18 and therefore has a structural wavelength corresponding to 20 degrees along the circumferences of the cylinder. Therefore, in the vicinity of ϕ=180^{o} where the two traveling waves have nearly the same magnitude, the velocity envelope has a periodic wave pattern but with a wavelength of 10^{o} along the circumference due to the interaction of the two waves traveling in opposite directions around the cylinder. Closer to the drive point the velocity profile becomes more complicated because of the greater contribution of the membrane modes to the total response. Figure 19 also shows the actual traveling wave pattern at a time "T" when the drive point response is at its maximum amplitude.

At frequencies above the ring frequency where the membrane modes have little or no effect upon the response, the velocity profile is less

complicated for a damping value of .01. This fact is illustrated in Figure 20 where the cylindrical shell in vacuo is point driven at a frequency corresponding to α=.5. For convenience, the maxima and minimum points of the velocity response are represented by an envelope as a function of the circumferential coordinate ϕ.

As the observation point moves further away from the drive point the envelope widens. The maximum width of the envelope would occur at ϕ=180 where the two traveling waves are of equal magnitude. However, closer to the drive point the standing wave pattern of the velocity envelope is less apparent since the response is primarily caused by the wave traveling the least distance from the drive point. For comparison purposes the response of a point excited plate with a structural damping value of .01 would tend to predict an average value for the cylinder's response in Figure 20.

Away from the drive point along the generator of the cylinder, interference of the waves traversing the cylinder also occurs. However, the effect of this interference on the response of the cylinder is always less than for a case where the waves circumscribe the cylinder at the drive point. This is because along the generator away from the drive point, the waves must follow a helical path to the observation point. The distance of the length of the helical path is always larger than $2\pi a$, the circumference of the cylinder. Consequently, due to damping, the effect of interference at the observation point is diminished.

SUMMARY

In this report an analysis has been presented for calculating the vibration response of a point excited, infinitely long, thin cylindrical shell immersed in an acoustic medium. Using the Fourier transform approach

and refined numerical techniques it was possible to obtain a direct solution without the inhibiting assumptions or approximations used in may previous studies. In order to verify the analysis to the best possible extent, results were compared with those of a fluid loaded, point excited plate at higher frequencies. The vibration response of the point driven plate was obtained by employing a numerical technique similar to the one used to obtain a solution for the cylinder.

Example calculations were performed for a cylinder with a wall thickness to radius ratio of .01. A comparison between the results for a point excited cylinder and plate has given additional insight into the frequency regions where a cylinder can be reasonably approximated by a plate (and where it cannot be). It was found, not unexpectedly, that the greatest difference between the responses of a point excited plate and cylinder occurs at low frequencies and also in the vicinity of the ring frequency of the cylinder where membrane type modes dominate. However, it was surprising how quickly the two responses approach each other above the ring frequency but well below the critical frequency of the plate ($\alpha \approx 1.0$). Consequently for the example presented, that is with an h/a ratio of .01, the response of a point excited cylinder can be approximated with reasonable accuracy by the response of a point excited plate in the mid frequency range ($\alpha \approx .5$) as well as at higher frequencies (of evaluation). It is very advantageous whenever the response of a cylinder can be approximated by a plate since the analysis of a plate is much easier and cheaper than for a cylinder.

Although the radiated pressure in the near field for the cylinder was not calculated, it can be done using Equation (25). The numerical method used to evaluate the pressure integrals would be identical to the one

developed to evaluate the response integrals. It would be interesting to compare the radiated pressure field of a point excited cylinder and plate, particularly in the frequency region where the membrane or extentional strains in the cylinder are of significance.

APPENDIX A

NORMALIZED RESPONSE OF A POINT EXCITED CYLINDRICAL SHELL

The results presented in this report have been normalized in two different ways. First of all, when investigating the behavior of individual circumferential modes, the response was normalized to the admittance of a line excited plate in vacuo. On the other hand, the total response, which contains all the circumferential modes of vibration, was normalized to the admittance of a point excited plate in vacuo.

NORMALIZING TO A POINT EXCITED PLATE

The expression, Equation (21a), for the response of a point excited cylindrical shell can be written in the follow form

$$\dot{w}(\phi,z,t) = \frac{F}{\rho_s c_p (2\pi a)^2} \sum_{n=0}^{\infty} \varepsilon_n \cos n\phi e^{-i\omega t} \int_{-\infty}^{+\infty} \frac{e^{i\bar{k}(z/a)} d\bar{k}}{Z_{ns}(\bar{k}) + Z_{na}(\bar{k})} \qquad \text{(A1)}$$

where $\bar{k} = ka$ (Nondimensionalized wave number)

$$\bar{Z}_{ns} = \frac{Z_{ns}}{\rho_s c_p} \quad \text{(Nondimensionalized shell impedance)}$$

$$Z_{na} = \frac{Z_{na}}{\rho_s c_p} \quad \text{(Nondimensionalized acoustic impedance)}$$

The drive point velocity of a point excited plate in vacuo is

$$v_v(0) = \sqrt{\frac{3}{4}} \frac{F}{\rho_s c_p h^2} \qquad \text{(A2)}$$

Dividing Equation (A1) by Equation (A2) the normalized cylinder response may be expressed as

$$\dot{\bar{w}}(\phi,z,t) = \frac{}{\sqrt{3}\,\pi^2}\left(\frac{h}{a}\right)^2 \sum_{n=0}^{\infty} \varepsilon_n \cos n\phi e^{-i\omega t} \int_{-\infty}^{+\infty} \frac{e^{i\bar{k}(z/a)}dk}{Z_{ns}(\bar{k}) + Z_{na}(\bar{k})} \qquad \text{(A3)}$$

NORMALIZING TO A LINE EXCITED PLATE

The drive point velocity of a line excited plate in vacuo without damping has an exact solution of the form

$$v_p(0) = \frac{F'k_p}{4\omega\rho_s h}(1 + i) \qquad \text{(A4)}$$

If Equation (A1) is divided through by $\frac{F'k_p}{4\omega\rho h}$, the normalized admittance of the nth mode for a point excited cylinder is given by

$$\dot{\bar{w}}_n(o,o,t) = \frac{2}{\pi}\left(\frac{h}{a}\right)(\Omega\beta)^{1/2}\,\varepsilon_n e^{-i\omega t} \int_{-\infty}^{+\infty} \frac{d\bar{k}}{Z_{ns}(k) + Z_{na}(k)} \qquad \text{(A5)}$$

where $F' = \frac{F}{2\pi a}$

Similarily, the normalized admittance for a line excited plate in vacuo is

$$\bar{v}_p(0) = 1 + i \qquad \text{(A6)}$$

APPENDIX B

HIGH FREQUENCY APPROXIMATION FOR A POINT EXCITED INFINITELY LONG CYLINDER IN VACUO

Heckl has obtained a high frequency approximation for the admittance of a point excited thin cylindrical shell in vacuo.[7] For a particular circumferential mode Heckl's expression is given by

$$\frac{1}{z_n} = \frac{i}{4\beta c_p \rho_s h} \left[\left(n^2 - \frac{\Omega}{\beta} \right)^{-1/2} - \left(n^2 + \frac{\Omega}{\beta} \right)^{1/2} \right] \tag{B1}$$

The above equation is presumably valid in the frequency region where $\Omega >> 1$. The admittance or drive point velocity of the shell can be expressed as

$$w(z=0,\phi=0) = \left(\frac{1}{\pi a} \right) \sum_{n=0}^{\infty} \frac{1}{z_n} \tag{B2}$$

In Figure 21 the high frequency approximation is compared with the admittance previously obtained for a point excited cylinder and plate. It is evident that Heckl's high frequency approximation converges to a point excited plate and is an excellent approximation to a cylinder in the frequency range of $\alpha \geq .5$ for a h/a ratio of .01. It is also interesting to note that for $\alpha = .5$, $\Omega = .7$ which indicates the above approximation is valid for frequencies much lower than originally assumed. However, it is apparent that Heckl's approximation neglects the membrane modes of the cylinder.

In the expression for admittance, Equation (B1), if $n^2 >> \frac{\Omega}{\beta}$ it can be shown that

$$\frac{1}{z_n} = \frac{i\Omega}{4\beta^2 c_p \rho_s h\, n^3} \tag{B3}$$

Thus for large n, $\frac{1}{z_n}$ is inversely proportional to n^3. This fact can be used to minimize truncation errors when calculating the admittance.

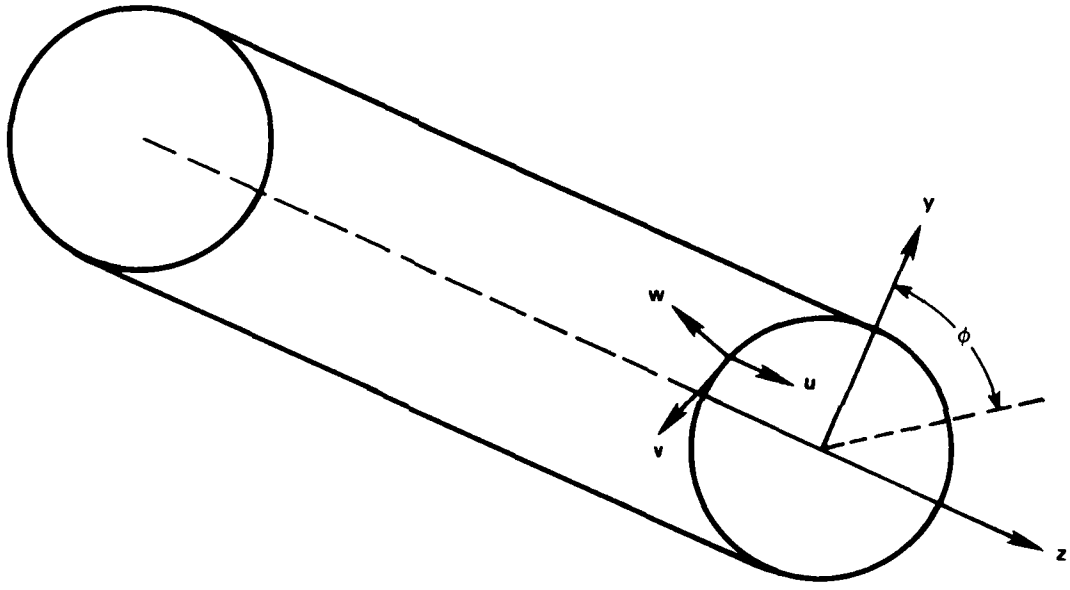

Figure 1 - Geometry of Cylindrical Shell
Showing Direction of Displacements

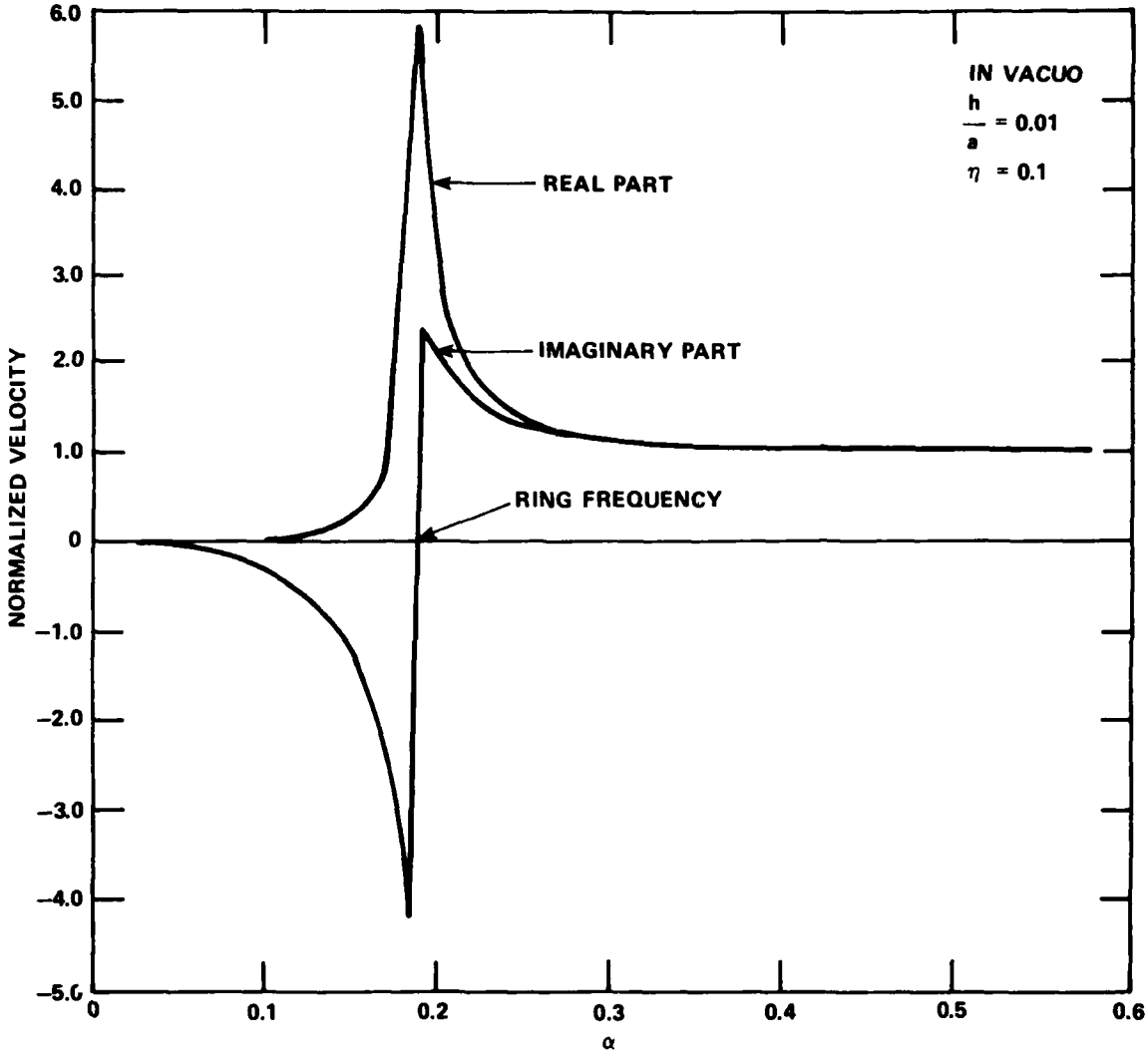

Figure 2 - Admittance of the Circumferential n=0 Mode for a Cylindrical Shell in Vacuo

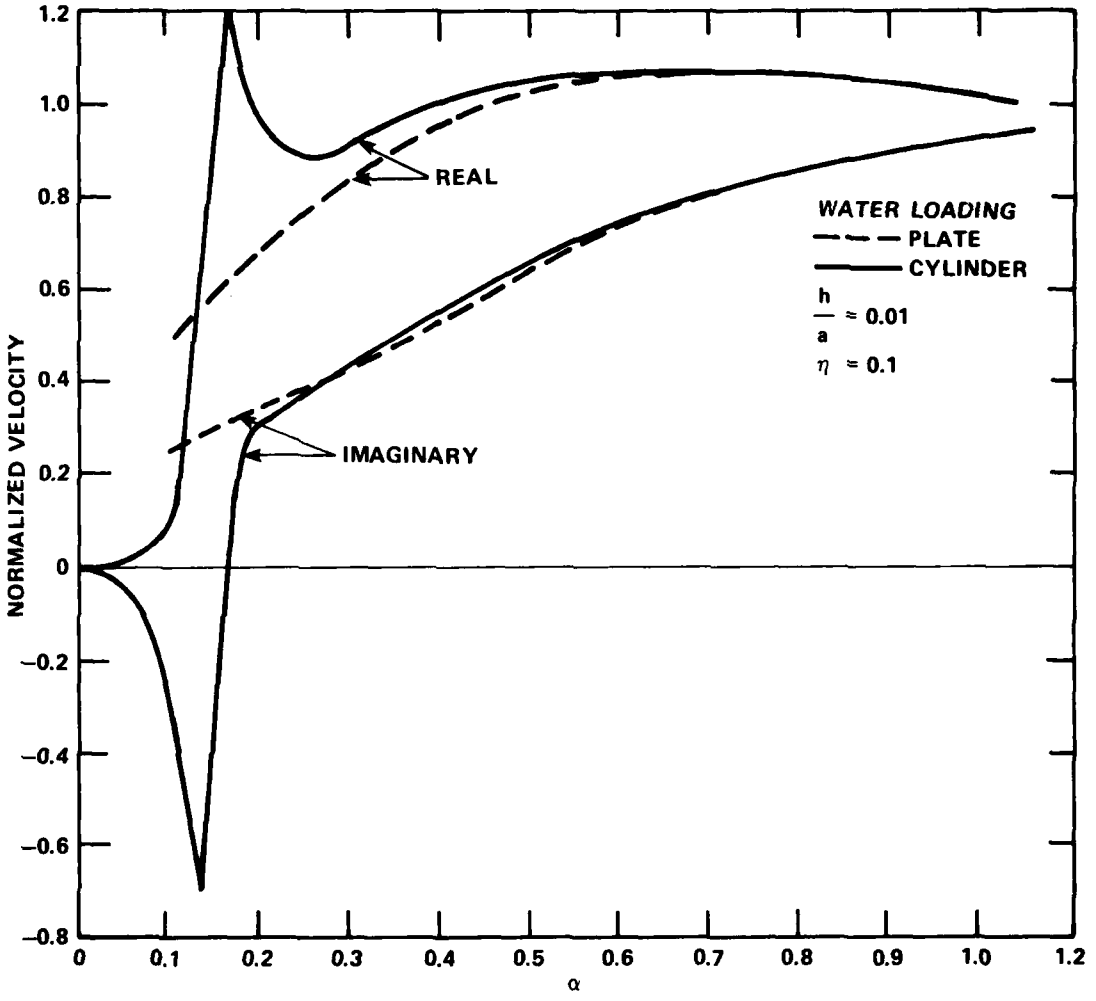

Figure 3 - Admittance of the Circumferential n=0 Mode for a Cylindrical Immersed in Water and a Plate with Water on One Side

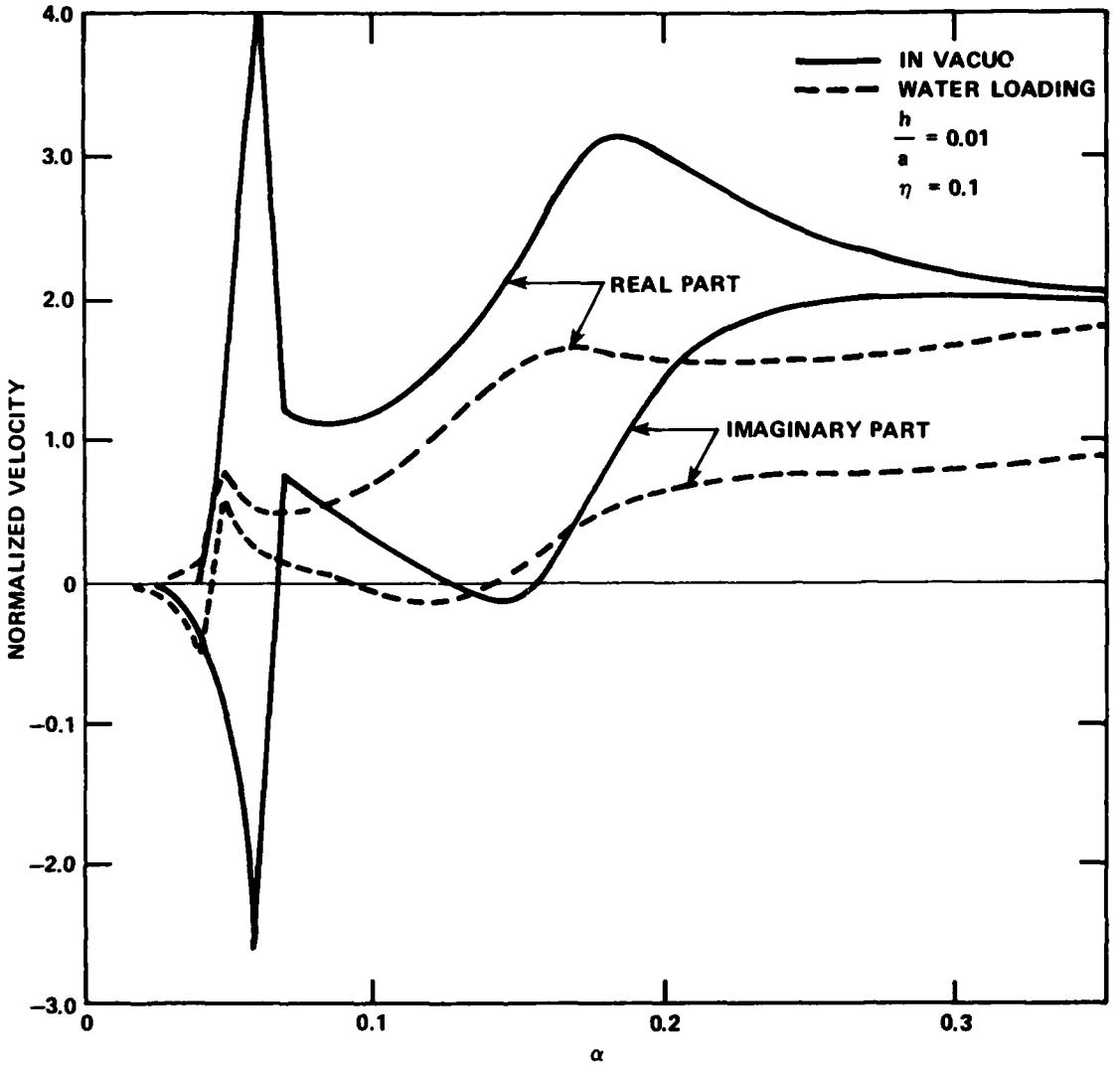

Figure 4 - Admittance of a Cylindrical Shell Immersed in Water and in a Vacuum for Circumferential Mode 6

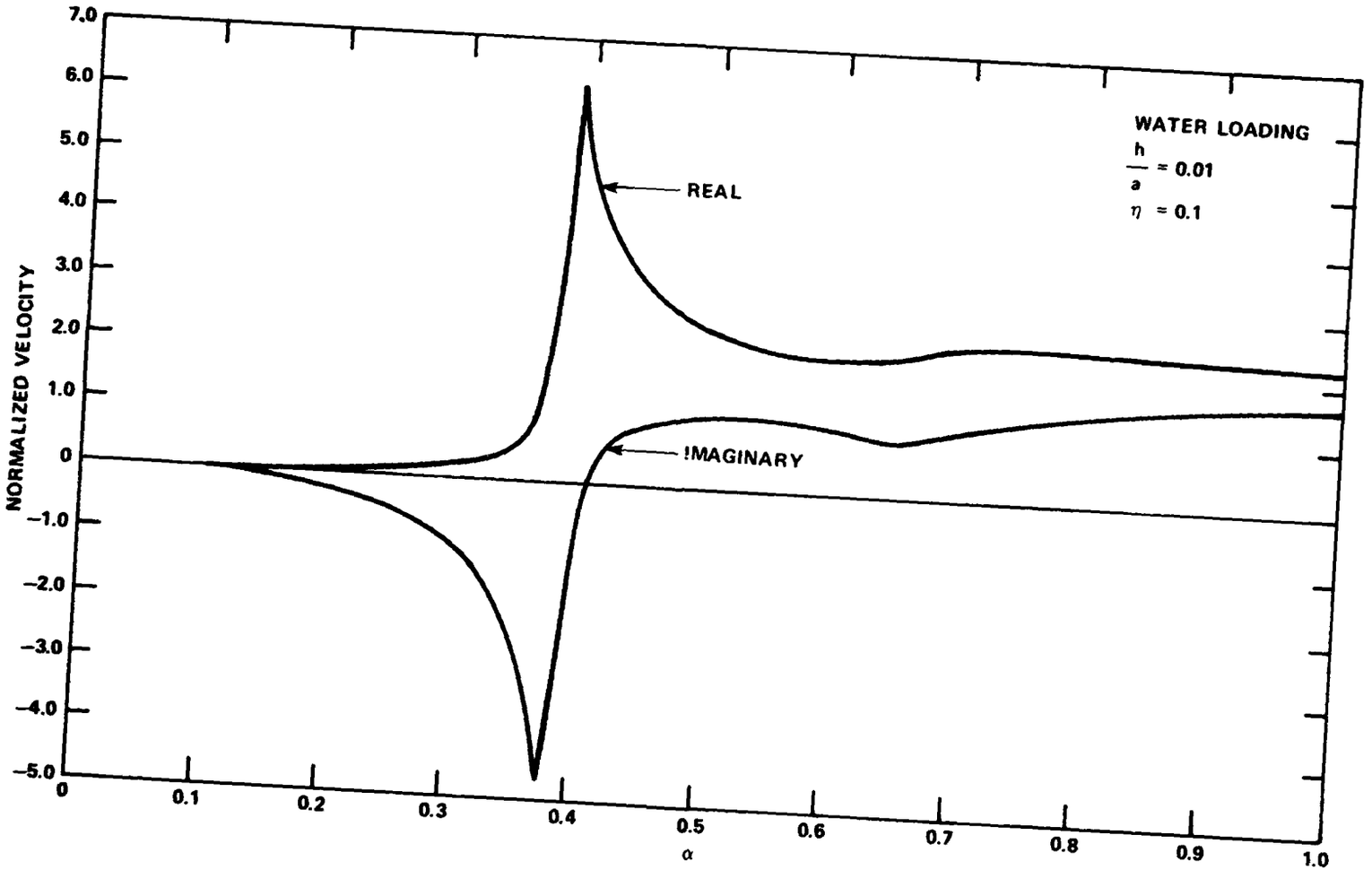

Figure 5 - Admittance of a Cylindrical Shell Immersed in Water for Circumferential Mode 41

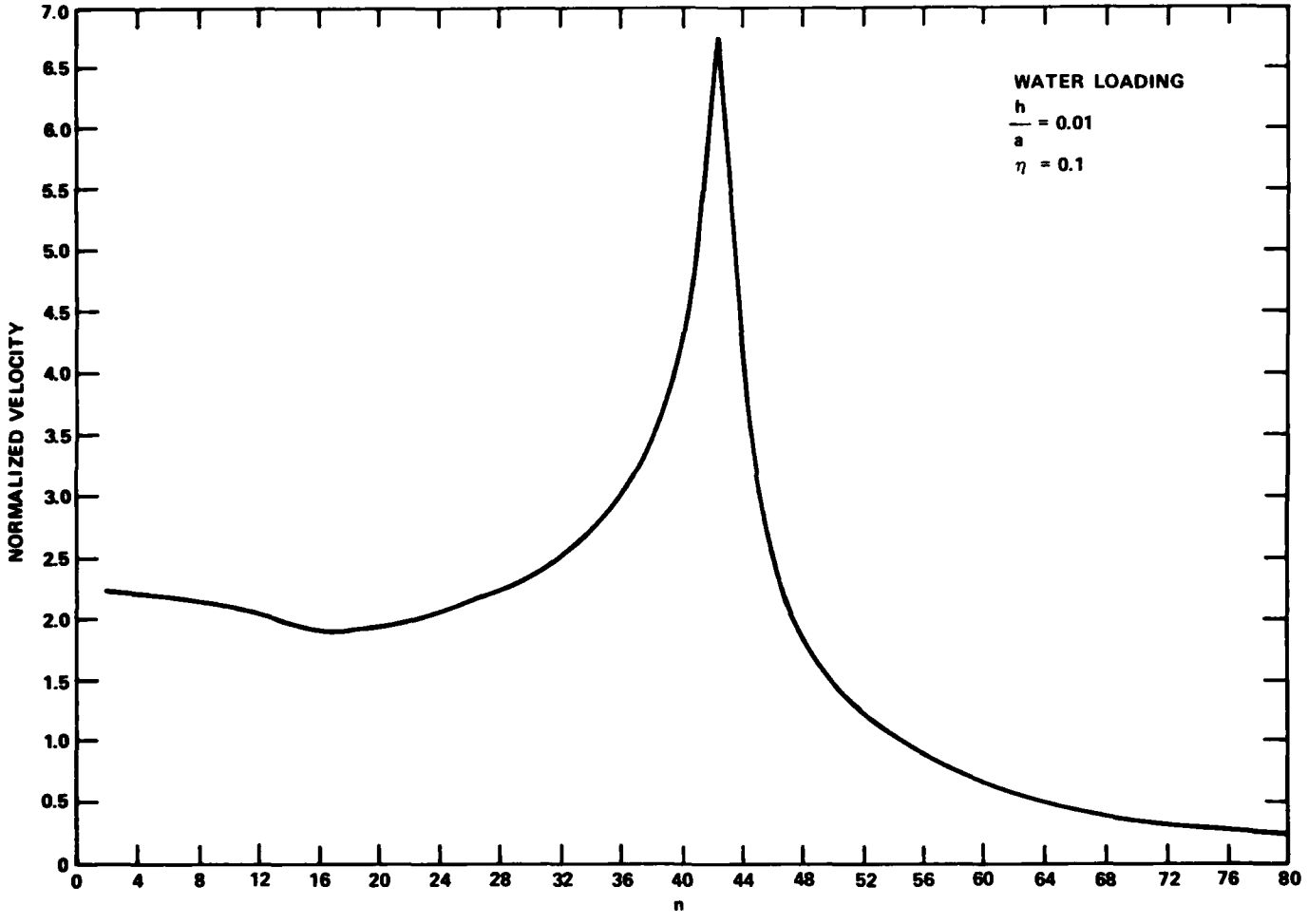

Figure 6 - Response of the Various Modes of Vibration for a Cylindrical Shell Immersed in Water and Excited at a Frequency Corresponding to the Forty First Circumferential Mode

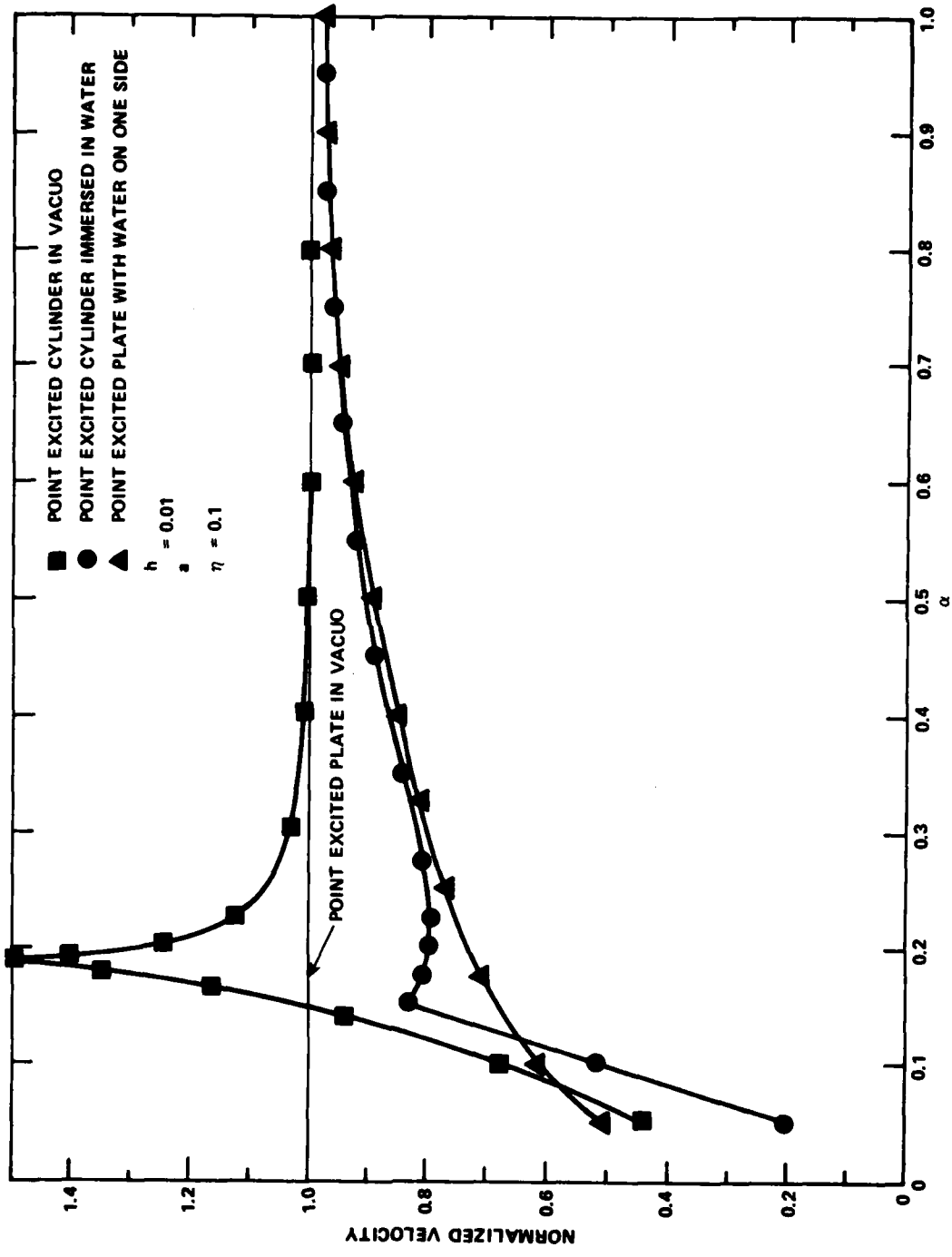

Figure 7 - Drive Point Velocity of a Cylindrical Shell and a Plate as a Function of Frequency

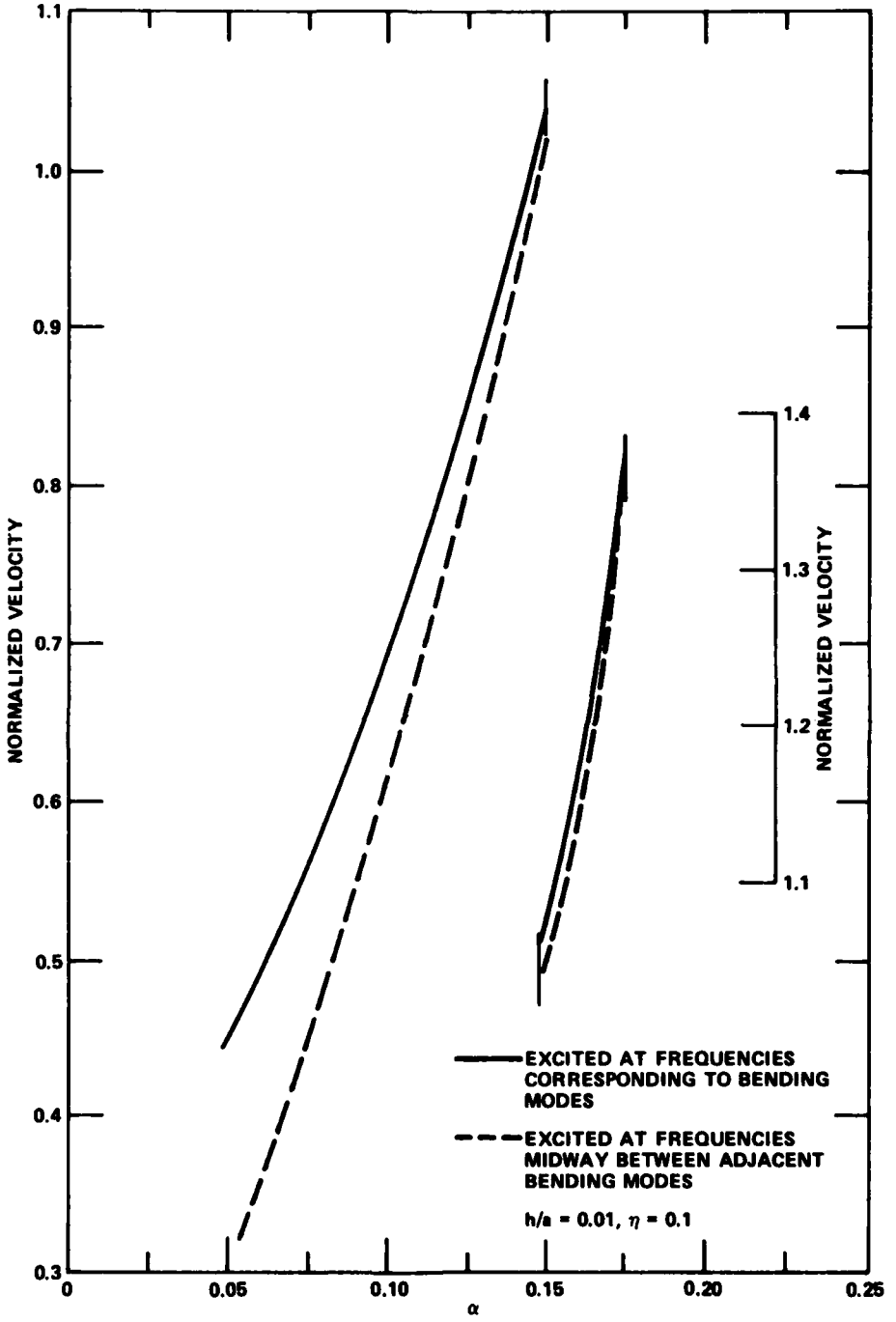

Figure 8 - Drive Point Velocity of a Cylindrical Shell in Vacuo at Low Frequencies

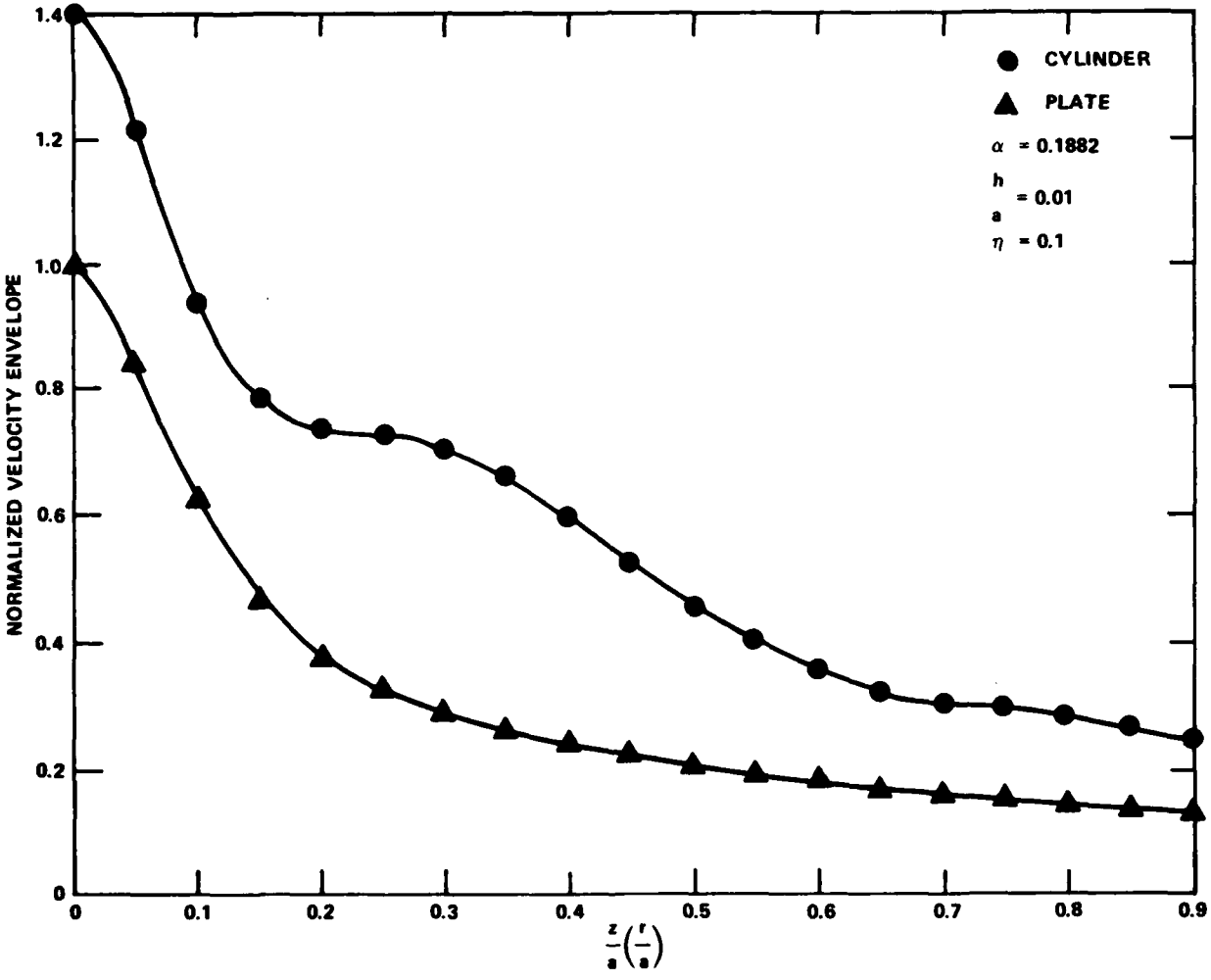

Figure 9 - Comparison of the Velocity Responses for a Cylinder and Plate in Vacuo, Point Excited at the Ring Frequency

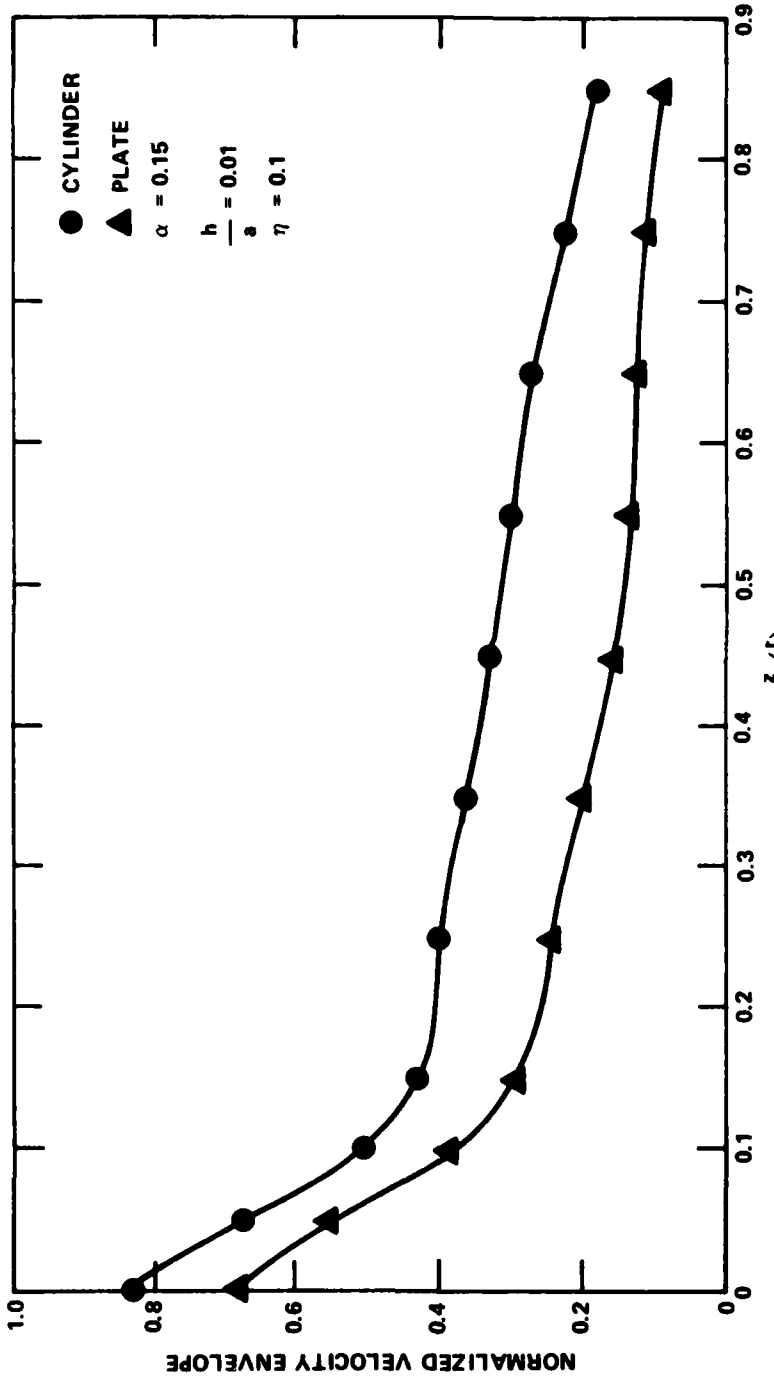

Figure 10 - Comparison of the Velocity Responses for a Cylinder and Plate in Water, Point Excited at the Ring Frequency

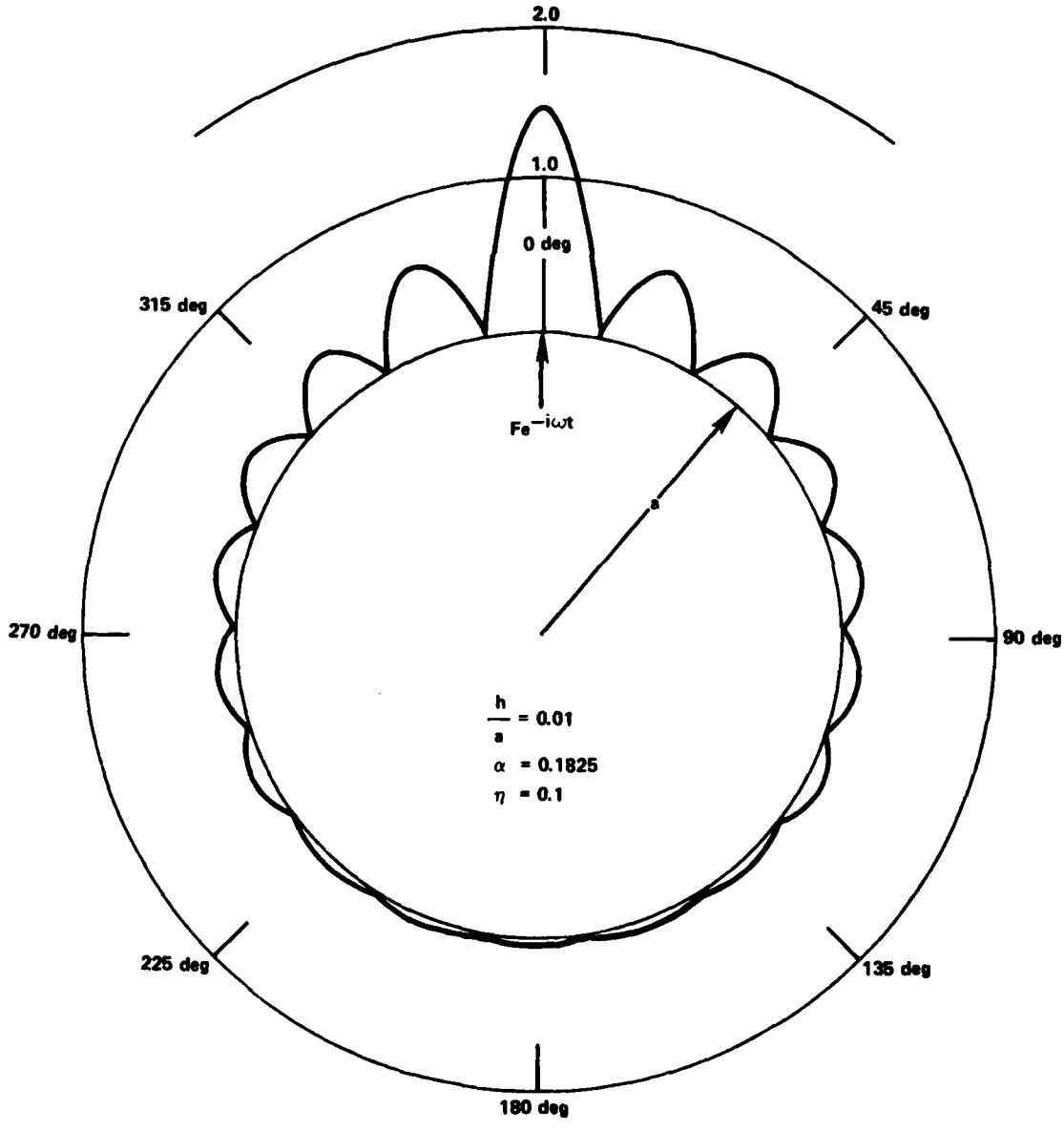

Figure 11 - Normalized Velocity Profile Along the Circumference of a Cylinder in Vacuo Point Driven at the Ring Frequency

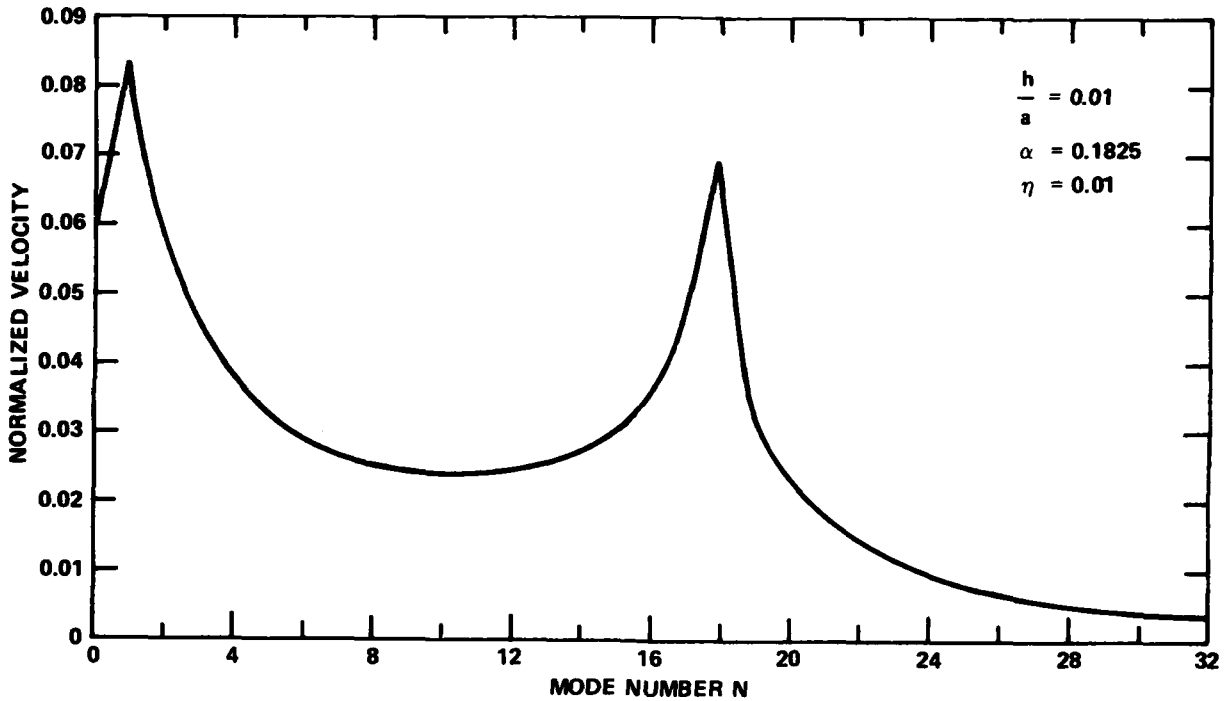

Figure 12 - Modal Response at the Drive Point for a Cylindrical Shell in Vacuo Excited at the Ring Frequency

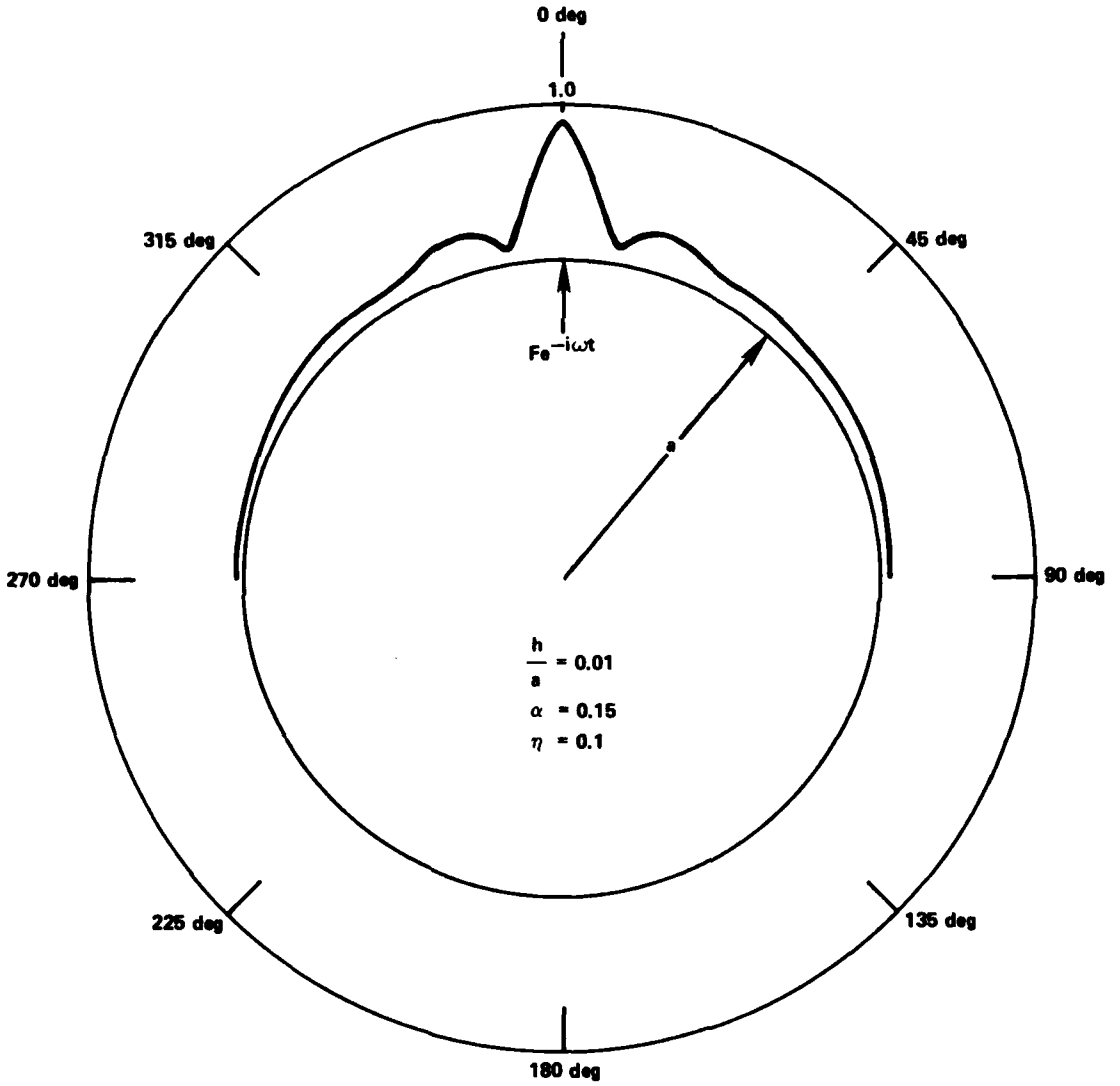

Figure 13 - Normalized Velocity Profile Along the Circumference of a Cylinder Immersed in Water Point Driven at the Ring Frequency

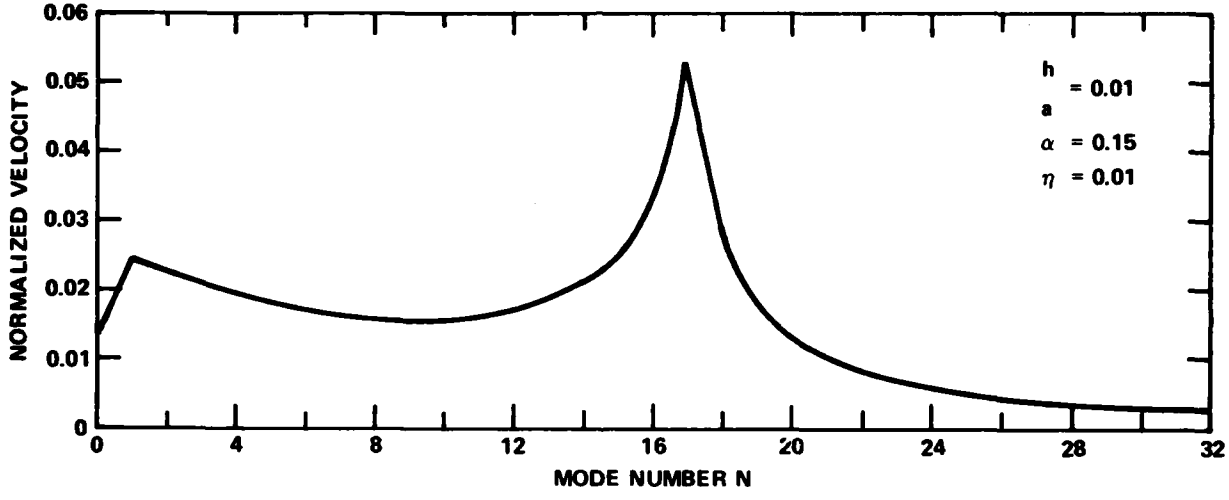

Figure 14 - Modal Response at the Drive Point for a Cylindrical Shell in Water Excited at the Ring Frequency

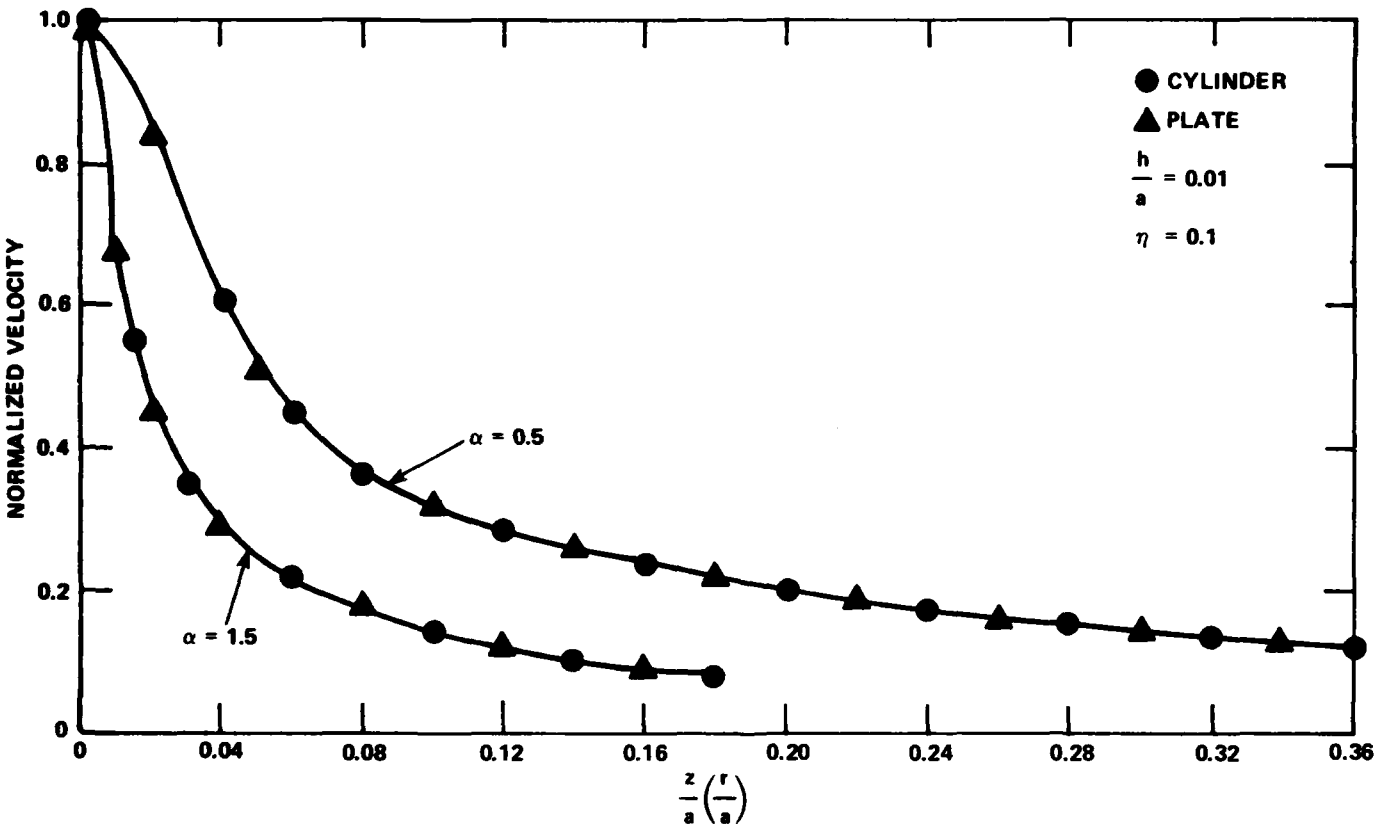

Figure 15 - Comparison of the Velocity Responses for a Cylinder and Plate in Vacuo, Point Excited at Frequencies of α=0.5 and α=1.5

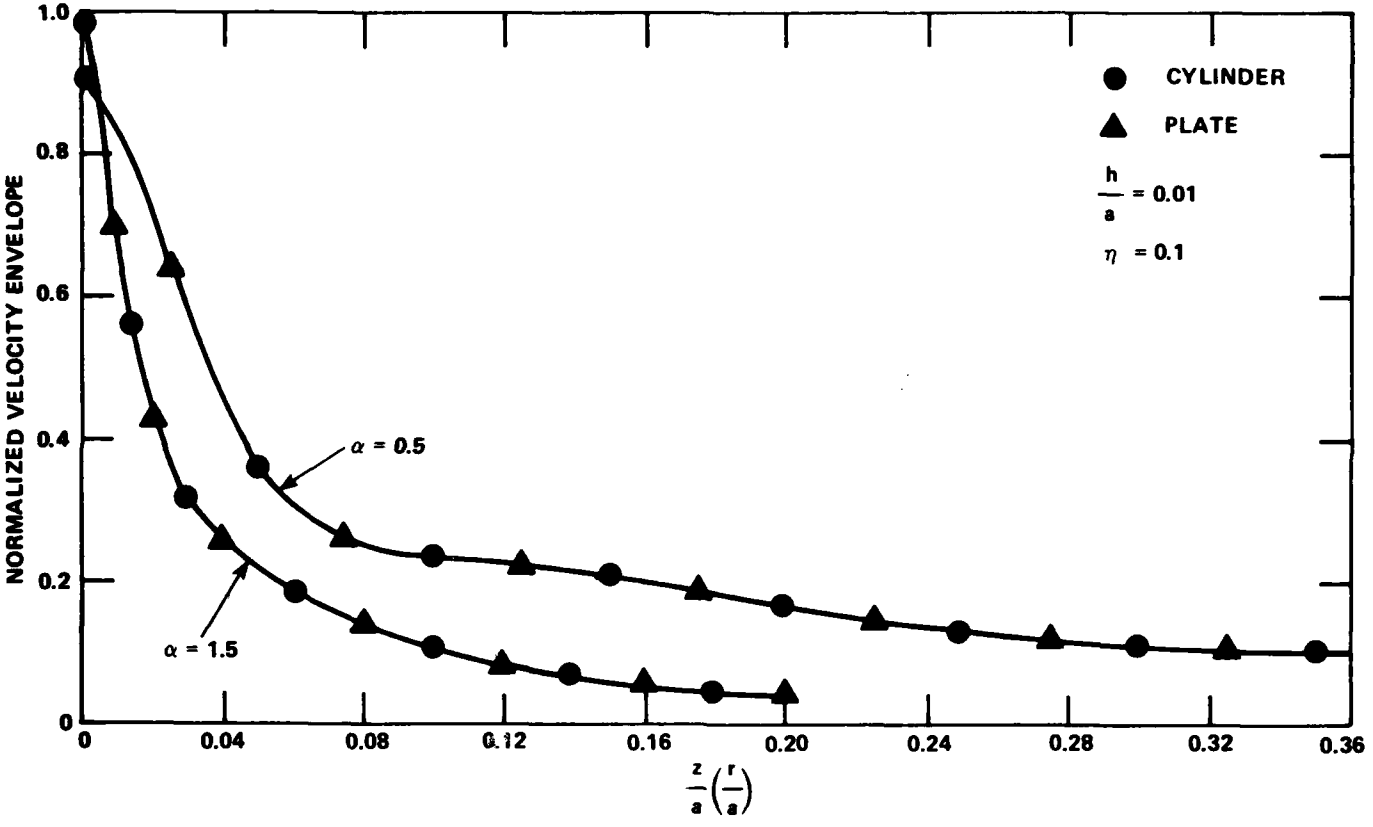

Figure 16 - Comparison of the Velocity Responses for a Cylinder and Plate in Water, Point Excited at Frequencies of α=0.5 and α=1.5

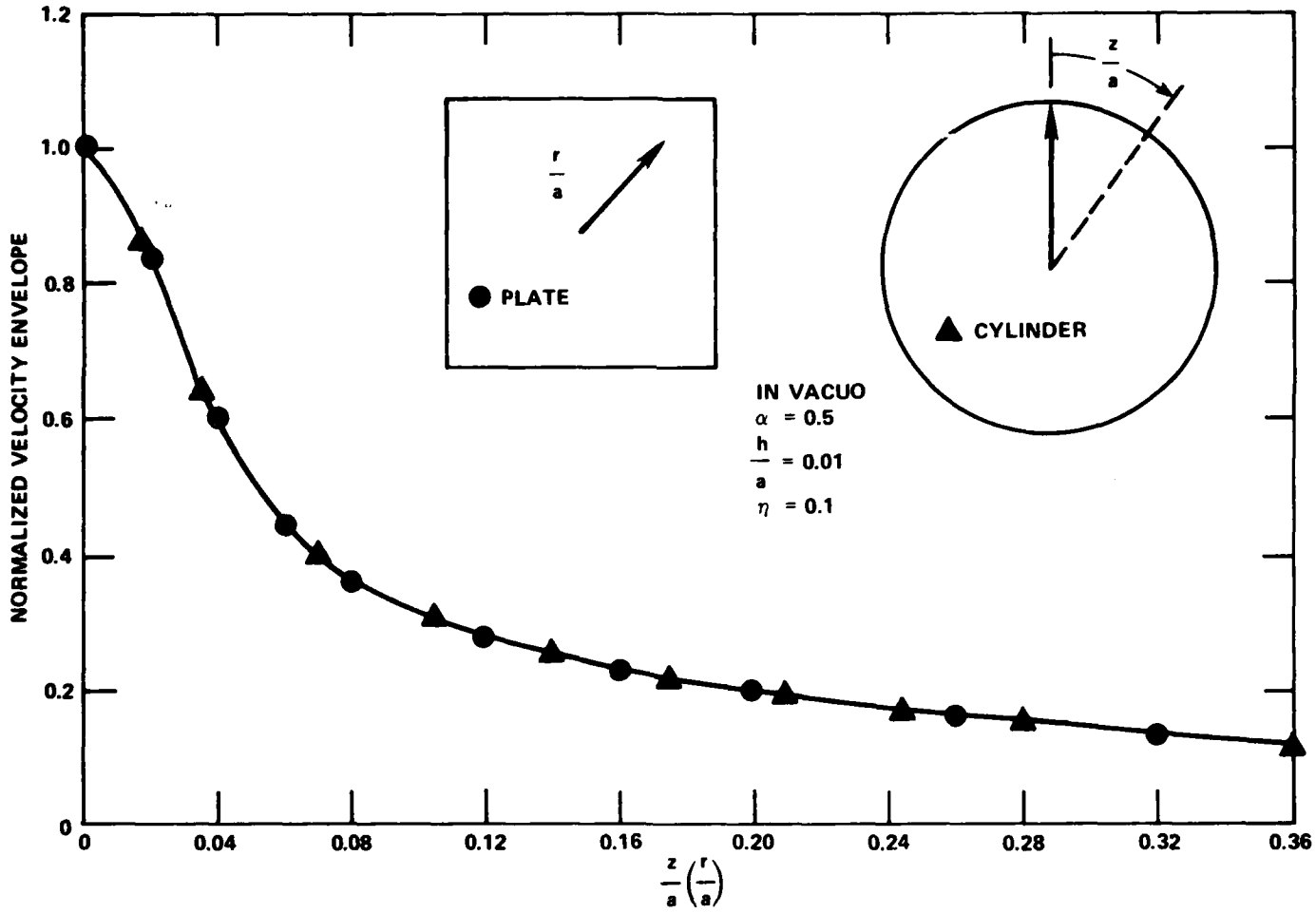

Figure 17 - Velocity Profile Along the Circumference of a Point Excited Cylinder Compared to the Velocity Profile for a Point Excited Plate

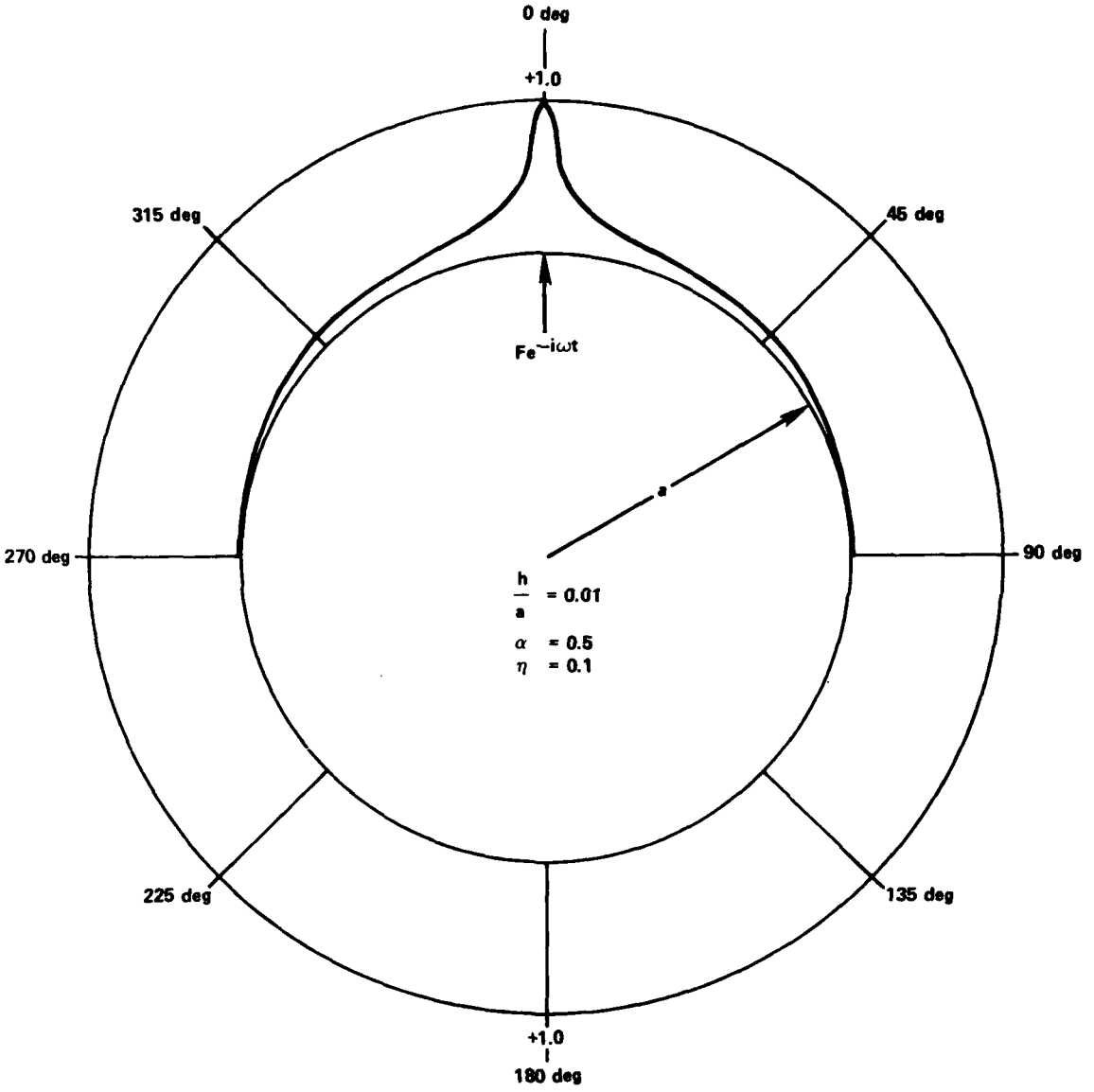

Figure 18 - Normalized Velocity Profile Along the Circumference of a Cylindrical Shell in Vacuo Point Driven at a Frequency of α=0.5

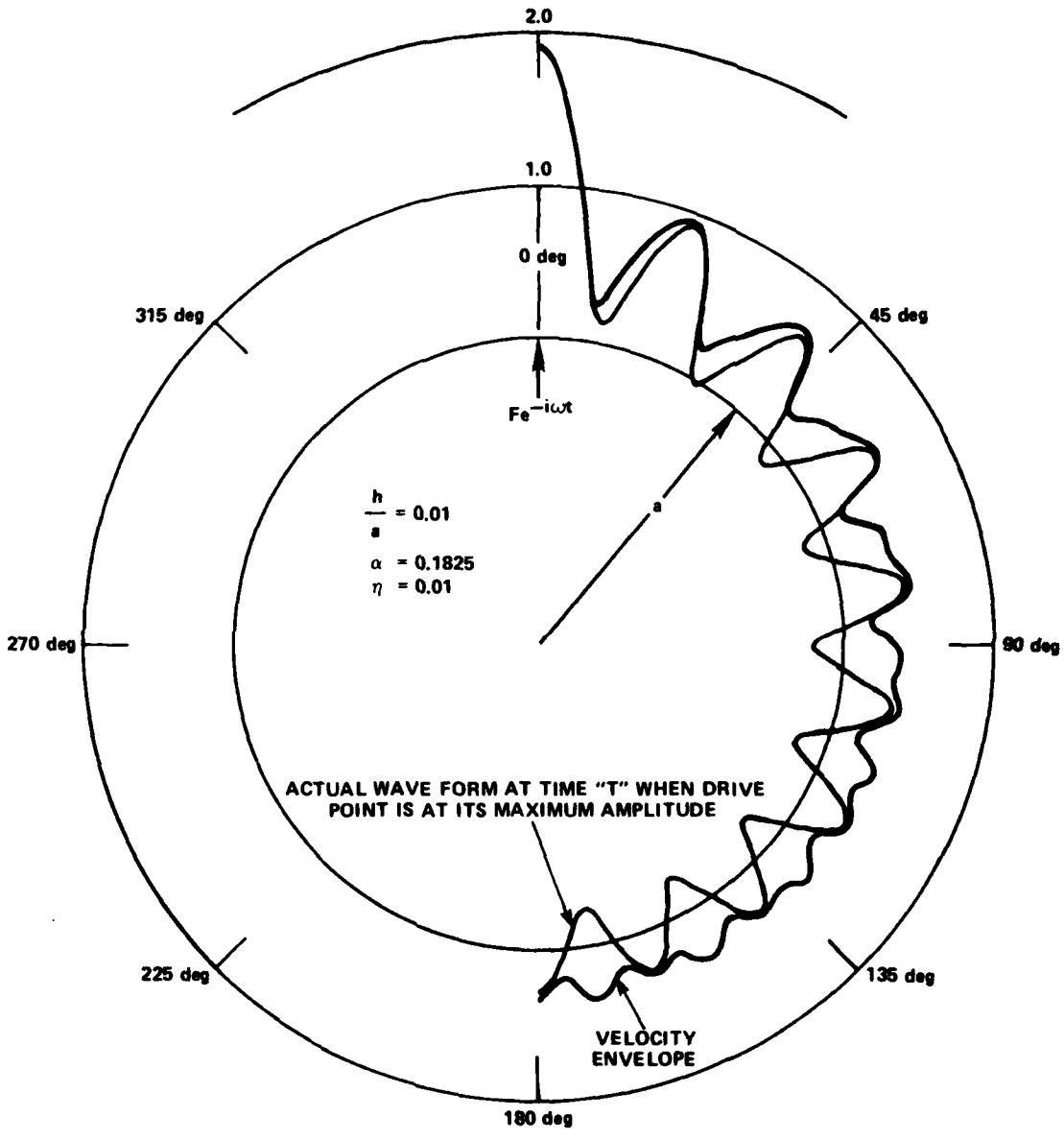

Figure 19 - Normalized Velocity Profile Along the Circumference of a Cylindrical Shell with a Structural Damping Value of 0.01 and Point Driven at the Ring Frequency in Vacuo

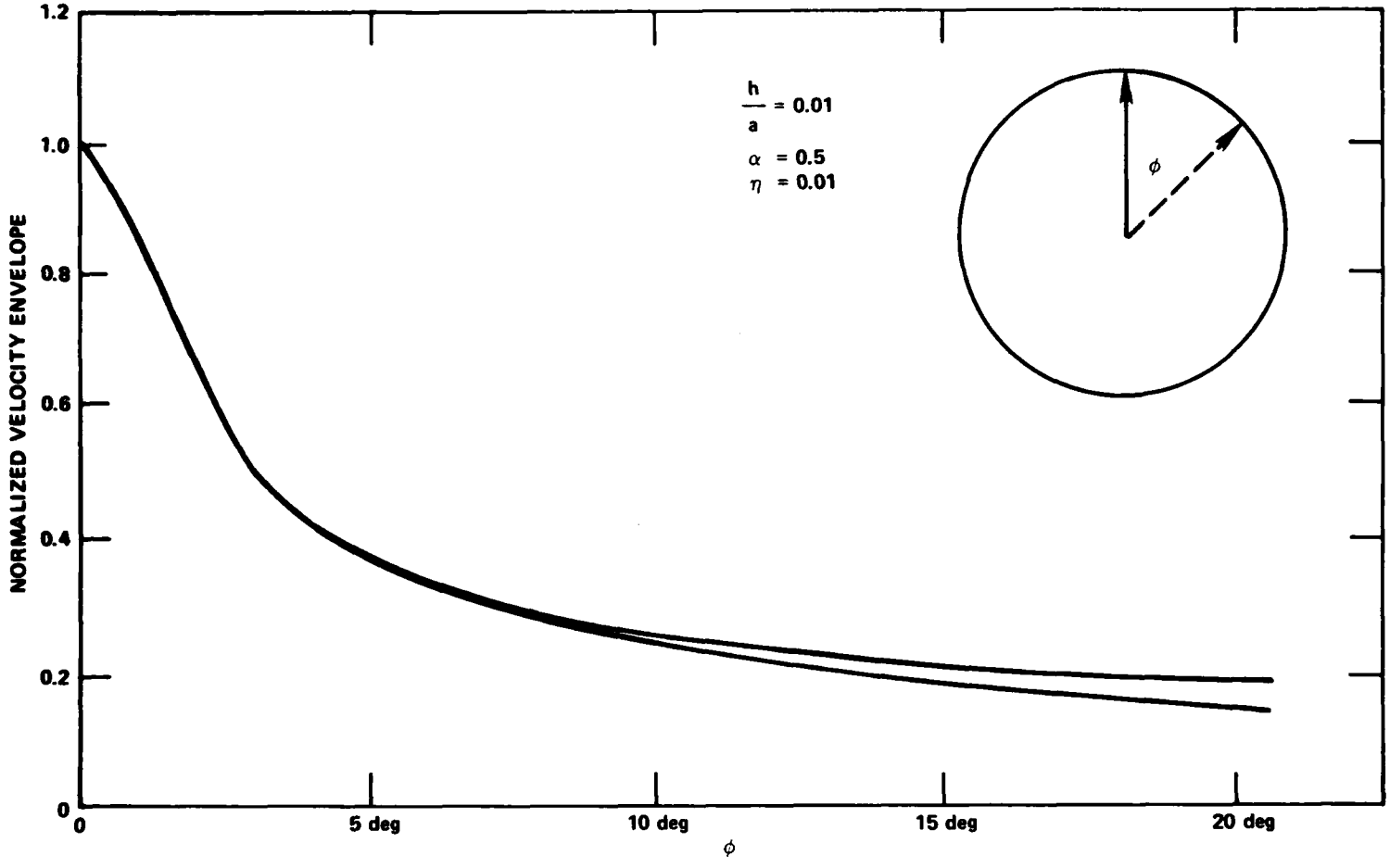

Figure 20 - Envelope of the Minima and Maxima Response of a Cylindrical Shell in Vacuo as a Function of the Circumferential Coordinate ϕ

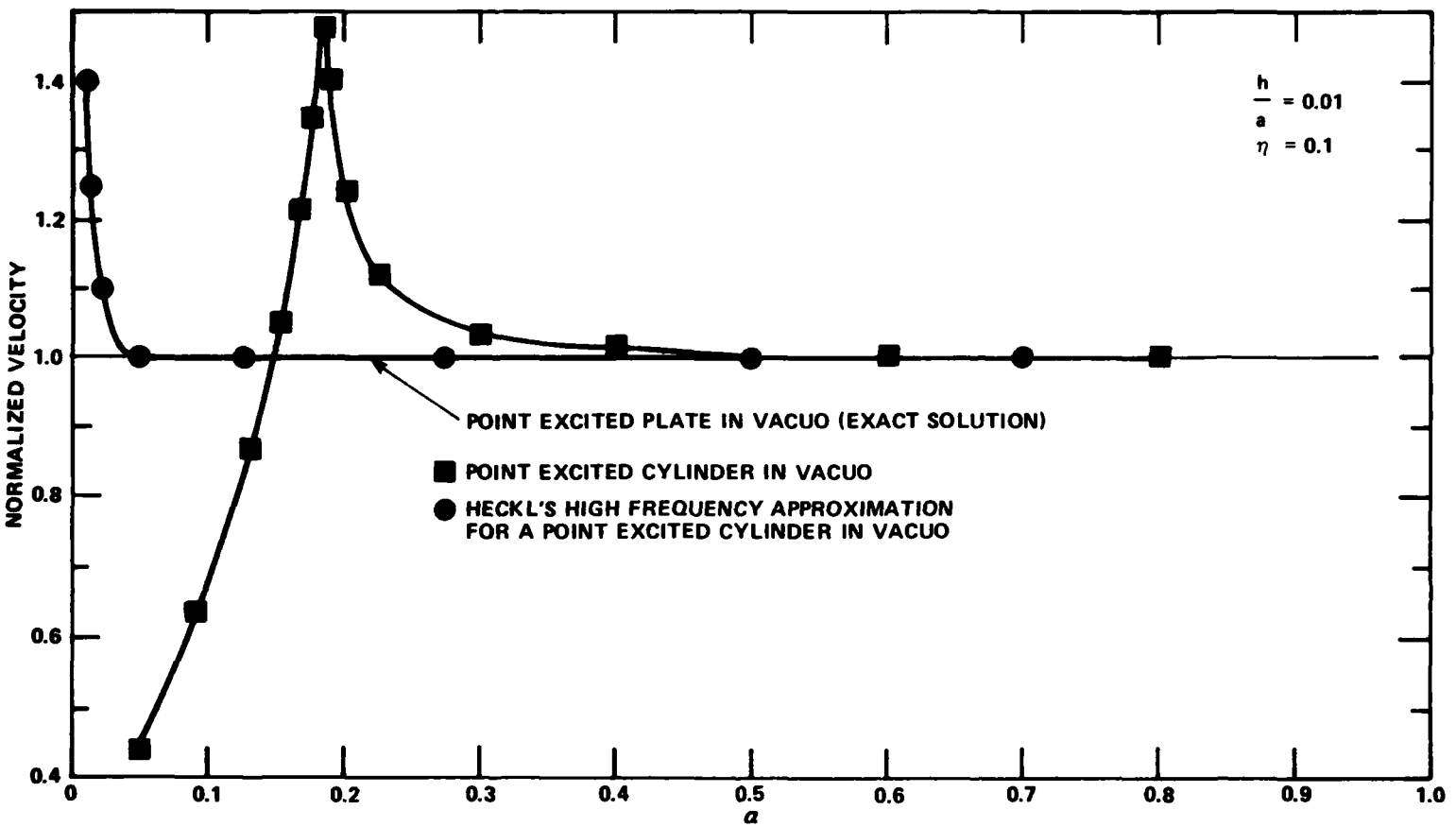

Figure 21 - Drive Point Velocity of a Cylindrical Shell and a Plate in Vacuo

REFERENCES

1. Junger, M. C., "Vibrations of Elastic Shells in a Fluid Medium and the Associated Radiation of Sound," Journal of Applied Mechanics, Trans. ASME, Vol. 19, pp. 439-445 (1952).

2. Bleich, H. H. and M. L. Baron, "Free and Forced Vibration of an Infinitely Long Cylindrical Shell in an Infinite Acoustic Medium," Journal of Applied Mechanics, Vol. 21, pp. 167-177 (1954).

3. Butler, Donald J., "Vibration of an Infinitely Long Cylindrical Shell in a Semi-Infinite Acoustic Medium," Journal of Ship Research, pp. 41-49 (Dec 1959).

4. Junger, M. C., "Dynamic Behavior of Reinforced Cylindrical Shells in a Vacuum and in a Fluid," Journal of Applied Mechanics, Vol. 21, pp. 35-41 (Mar 1954).

5. Junger, M. C. and D. Feit, "Sound, Structures, and Their Interaction," The MIT Press, Cambridge, Massachusetts (1972).

6. Warburton, G. B., "Vibration of a Cylindrical Shell in an Acoustic Medium," Journal Mechanical Engineering Science, Vol. 3, No. 1 (1961).

7. Heckl, Manfred, "Vibration of Point-Driven Cylindrical Shells," Journal of the Acoustical Society of America, Vol. 30, No. 10, pp. 1553-1557 (Oct 1962).

INITIAL DISTRIBUTION

Copies	
1	ONR 439
1	NRL/Washington
1	NUSC/New London
2	NAVSEA 2 SEA 05H
3	Penn State U/ARL 1 Hayek 1 Skudrzyk 1 Stuart
1	Penn State U/Neubert
1	Bolt Beranek & Newman/ Gorman
1	Cambridge Acoust Assoc/ Garrelick
12	DTIC

CENTER DISTRIBUTION

Copies	Code	Name
1	012	
1	1170	D. Jewell
1	1730.5	M. Critchfield
1	19	M. Sevik
1	1900	T. Eisler
1	1901	M. Strasberg
1	1902	G. Maidanik
1	1905.1	W. Blake
1	1905.2	W. Reader
1	1905.3	R. Cantrell
1	1905.4	D. Vendettis
1	192	R. Biancardi

CENTER DISTRIBUTION (Continued)

Copies	Code	Name
1	1926	K. Jones
1	194	J. Shen
1	1940	R. Waterhouse
3	196	D. Feit
1	1962	R. Brown
1	1962	W. Fontaine
1	1962	A. Kilcullen
1	1962	A. Zaloumis
1	1965	H. Ali
1	1965	J. Brooks
1	1965	J. Caspar
1	1965	F. Desiderati
1	1965	J. Goodman
1	1965	Y-N Liu
1	1965	J. Niemiec
1	1965	M. Rumerman
1	1965	S. Solomon
1	1965	A. Tucker
20	1965	W. Vogel
1	2740	Y. Wang
10	5211.1	Reports Distribution
1	522.1	Unclass Lib (C)
1	522.2	Unclass Lib (A)